

Development of an Electrochemical Surface Enhanced Raman Spectroscopy (EC-SERS) Fabric
Sensor to Detect Cortisol for Early Diagnosis of Post-Traumatic Stress Disorder

By
Jaskaran Singh Anand

A Thesis Submitted to
Saint Mary's University, Halifax, Nova Scotia
in Partial Fulfillment of the Requirements for
the Degree of Bachelor of Science with Honours in Biology.

April 2022, Halifax, Nova Scotia

Copyright [Jaskaran Singh Anand, 2022]

Approved: Dr. Christa Brosseau
Supervisor

Approved: Dr. Genlou Sun
Reader

Date: April 27, 2022

Development of an Electrochemical Surface Enhanced Raman Spectroscopy (EC-SERS) Fabric
Sensor to Detect Cortisol for Early Diagnosis of Post-Traumatic Stress Disorder

by
Jaskaran Singh Anand

ABSTRACT

Early diagnosis of Post-Traumatic Stress Disorder (PTSD) is challenging. Its prevalence rate in Canada is 9.2%. Experiencing stress for a sustained period can lead to a prolonged release of cortisol that causes negative feedback which leads to an eventual decrease in cortisol levels in PTSD patients. Electrochemical Surface Enhanced Raman Spectroscopy (EC-SERS) deals with enhancement of metal nanoparticles under application of voltage to detect the analyte signal. EC-SERS is advantageous for detecting biological samples. Here we report using blend fabric (37% silk, 35% hemp, 28% organic cotton) for the development of a functional fabric sensor using EC-SERS to detect cortisol for early diagnosis of PTSD. Cortisol is a glucocorticoid stress hormone and a challenging molecule to be detected with EC-SERS. The fabric sensor is comprised of a counter electrode, reference electrode, and working electrode. The counter electrode and working electrode are printed on fabric with carbon ink on top of silver ink and the reference electrode is imprinted on fabric with silver conductive ink. To provide effective SERS enhancement, silver nanoparticles were deposited on the working electrode area. For proof-of-concept studies, a 1 mg/mL analytical standard of cortisol in methanol was used for these investigations. Cortisol signal increased with an increase in the application of negative voltage. Quantitative analysis of signal intensity with cortisol concentration was also evaluated. To determine the relationship between peak intensity and analyte concentration, EC-SERS studies were conducted with 50 μL , 65 μL , 75 μL , and 100 μL of 1 mg mL⁻¹ cortisol. In summary, a fabric-based EC-SERS sensor for the detection of cortisol was demonstrated, paving the way to a wearable sensor for early PTSD diagnostics.

April 27, 2022

ACKNOWLEDGEMENTS

Firstly, I would like to thank the National Research Council for providing funding for this honours research project through the NRC New Beginnings Research Fund. I would like to thank Dr. Christa Brosseau for guiding me throughout my undergraduate honours research project, being patient and empathetic with me. I would also like to thank Dr. Genlou Sun for reading my thesis and providing appropriate feedback. I would also like to thank Dr. Timothy Frasier and Dr. David Chiasson for all the feedback, information and contributions that was provided in the honour's seminar class as well as my class members for peer reviewing my thesis drafts. I also thank Dr. Li-Lin Tay from the National Research Council. I would also like to thank my lab members for their support and training me with the experiments. At last, I would like to thank Xiang Yang for his assistance with imaging the fabric samples.

Finally, I would like to thank the Department of Biology and Department of Chemistry for inspiring me to challenge myself and do honours in Biology. I am grateful to all of those who I had pleasure to work during this project.

Last but not the least, I would like to thank my family and friends for their continuous support and for being there for me when needed. Thanks to everyone who helped me accomplish this achievement.

Table of Contents

ABSTRACT	Error! Bookmark not defined.
ACKNOWLEDGEMENTS	III
LIST OF TABLES	VI
LIST OF FIGURES	VII
LIST OF ABBREVIATIONS	IX
1 INTRODUCTION	1
1.1 Post-Traumatic Stress Disorder (PTSD) and its Causes and Symptoms	1
1.2 Diagnostic and Treatment of PTSD	2
1.3 Biomarkers for PTSD	3
1.3.1 Cortisol	4
1.3.2 Dehydroepiandrosterone	6
1.4 Electrochemical Surface-Enhanced Raman Spectroscopy (EC-SERS)	8
1.5 Point-of-Care Diagnostics	10
1.6 Wearable Sensors	11
1.7 Advancements in Wearable Sensors	12
1.8 Fabric Electrodes	15
1.9 Study Objective	16
2 MATERIAL AND METHODS	17
2.1 Reagents and Solutions	17
2.2 Instrumentation	17
2.3 Synthesis of Silver Nanoparticles	18
2.4 Preparation of EC-SERS Sensors	19
2.4.1 Preparation of Screen-Printed Electrodes.....	19
2.4.2 Preparation of fabric electrodes	19
2.5 Electrochemistry	21
2.6 EC-SERS Studies	22
2.6.1 EC-SERS studies with Cortisol on Fabric Sensor	22
3 RESULTS AND DISCUSSION	25
3.1 Characterization of Silver Nanoparticles (AgNPs)	25
3.1.1 UV-vis Spectroscopy of AgNPs	25
3.1.2 Scanning Electron Microscopy (SEM)	26
3.2 Fabrication and Characterization of EC-SERS sensors	27

3.2.1	Fabrication and Characterization of the Fabric Chip Electrode.....	27
3.2.2	Electrochemistry	31
3.3	EC-SERS of Cortisol	32
3.3.1	EC-SERS for cortisol on the fabric sensor	32
4	CONCLUSION AND FUTURE WORK	53
5	APPENDIX	56
5.1	Copyright of Figures Used.....	56
5.2	Appendix Tables.....	57
6	REFERENCES.....	62

LIST OF TABLES

List of Tables	Page
Table 1. Clinical concentrations of Dehydroepiandrosterone found in human body. The DHEA levels vary with the age of an individual (Soldin et al. 2011).	7
Table 2. Peaks reported for 50 μL of 1mg mL^{-1} cortisol in cathodic region and -0.7 V vs Ag/AgCl. These peaks are consistent with the reported Raman peaks (Cortisol-Raman-Spectrum-Spectrabase) and SERS peaks for cortisol (Moore and Sharma 2020).	40
Table 3. Peaks reported for 50 μL of 1mg/mL cortisol in anodic region and -0.8V vs Ag/AgCl. These peaks are consistent with the reported Raman and SERS peaks for cortisol(Moore and Sharma 2020) (Cortisol-Raman-Spectrum-Spectrabase).	41
Appendix Table A1. For 20 silver nanoparticles, measured diameter reported along with its mean and standard deviation.	57
Appendix Table 2. Calculated difference between y-axis value and baseline value for the reported cortisol peaks in (A) Cathodic progression (B) -0.7V vs Ag/AgCl of cathodic progression (C) -0.8V vs Ag/AgCl of cathodic progression (D) Anodic progression € -0.8V vs Ag/AgCl of anodic progression	58
Appendix Table 3. Coefficient of variation and standard deviation value for the intensity of reported 50 μL of 1.0 mg mL^{-1} cortisol peaks	61

LIST OF FIGURES

List of Figures	Page
Figure 1. Molecular structure of cortisol hormone, one of the biomarkers focused for early diagnosis of PTSD. Chemdraw software was used to draw the molecular structure of Cortisol.	5
Figure 2. Molecular structure of Dehydroepiandrosterone hormone, one of the biomarkers focused for early diagnosis of PTSD. Chemdraw software was used to draw the molecular structure of Dehydroepiandrosterone.	6
Figure 3. Washable and reusable SERS membranes textiles. The reactive ion etching treatment is used to expose the hotspots. SERS textile can be reused by washing of the Au NP wearable sensors in normal detergent with ultrasound sonication and mechanical stirring to remove analyte and contaminants from the hotspot.(Garg et al. 2020) (Reproduced with permission).	13
Figure 4. SERS wearable sensor with sweat absorption dermal protective layer. (A) illustrates a schematic representation of the wearable sensor patch used to perform EC-SERS for detecting drug molecules in sweat. (B) illustrates the composition of a wearable sensor patch which is biocompatible with skin. (Koh et al. 2021) (Reproduced with permission).	14
Figure 5. Assembly of a wearable sensor designed to detect cortisol. (A) Illustration of the design of the wearable sensor. (B) The medical tape is perforated using a bayonet microneedle derma pen. (C) describes the working fabric sensor being worn by an individual (Mugo and Alberkant 2020) (Reproduced with permission).	15
Figure 6. Fabric sensor showing reference electrode traced with silver conductive ink and carbon electrode, working electrode traced with carbon inductive ink.	21
Figure 7. EC-SERS set up for fabric electrode drawn using chemix software. The fabric electrode is connected to the potentiostat through cables. The Raman spectrometer is connected to a computer and the sample is analyzed using a 180° backscattering configuration.	23
Figure 8. UV-vis extinction spectroscopy of the colloidal silver nanoparticles used in this research.	25
Figure 9. SEM image of silver nanoparticles observed at a magnification of 200kx.	26
Figure 10. Fabric sensor showing reference electrode traced with silver conductive ink and carbon electrode, working electrode traced with carbon inductive ink.	28
Figure 11. Cathodic EC-SERS progression for 10 μ L of 1.0 mM p-ATP deposited on the fabric chip electrode. The spectra were acquired at 785 nm excitation for 30 seconds at a laser power of 42.6 mW.	29
Figure 12. EC-SERS spectrum at -0.9 V vs Ag/AgCl for 10 μ L of 1.0 mM p-ATP deposited onto the fabric chip electrode. The spectrum was acquired at 785 nm excitation for 30 seconds at a laser power of 42.6 mW.	30
Figure 13. Anodic EC-SERS progression for 10 μ L of 1.0 mM p-ATP deposited on the fabric chip electrode. The spectra were acquired at 785 nm excitation for 30 seconds at a laser power of 10.6 mW.	30

Figure 14. EC-SERS spectrum at -0.8 V vs Ag/AgCl for 10 μL of 1.0 mM p-ATP deposited onto the fabric chip electrode. The spectrum was acquired at 785 nm excitation for 30 seconds at a laser power of 42.6 mW.	31
Figure 15. Cyclic voltammetry (CV) plot showing the first and last cycle for the fabric sensor. Supporting electrolyte: 0.1 M NaF, Sweep rate: 50 mV s^{-1} .	32
Figure 16. (a) Cathodic (b) Anodic EC-SERS progression for 30 μL of 1.0 mg mL^{-1} cortisol deposited on the fabric chip electrode. The spectra were acquired at 785 nm excitation for 30 seconds at a laser power of 42.6 mW.	34
Figure 17. Cathodic EC-SERS progression for 50 μL of 1.0 mg mL^{-1} cortisol deposited on the fabric chip electrode. The spectra were acquired at 785 nm excitation for 30 seconds at a laser power of 42.6 mW.	37
Figure 18. EC-SERS spectra at -0.7V vs Ag/AgCl for 50 μL of 1 mg mL^{-1} cortisol deposited onto the fabric chip electrode. The spectrum was acquired at 785 nm excitation for 30 seconds at a laser power of 42.6 mW.	38
Figure 19. Anodic EC-SERS progression for 50 μL of 1.0 mg mL^{-1} cortisol deposited on the fabric chip electrode. The spectra were acquired at 785 nm excitation for 30 seconds at a laser power of 42.6 mW.	39
Figure 20. Comparison of OCP and -0.7 V Ag/AgCl signal peaks for 50 μL of 1.0 mg mL^{-1} cortisol deposited on the fabric chip electrode. The spectra were acquired at 785 nm excitation for 30 seconds at a laser power of 42.6 mW.	42
Figure 21. Cathodic EC-SERS progression for 50 μL of 1.0 mg mL^{-1} cortisol deposited on the fabric chip electrode. The spectra were acquired at 785 nm excitation for 30 seconds at a laser power of 42.6 mW.	43
Figure 22. Anodic EC-SERS progression for 50 μL of 1.0 mg mL^{-1} cortisol deposited on the fabric chip electrode. The spectra were acquired at 785 nm excitation for 30 seconds at a laser power of 42.6 mW.	44
Figure 23. Comparison of EC-SERS progression at -0.7V Ag/AgCl for 50 μg of 1.0 mg mL^{-1} cortisol trials deposited on the fabric chip electrode. The spectra were acquired at 785 nm excitation for 30 seconds at a laser power of 42.6 mW.	44
Figure 24. (a) Cathodic (b) Anodic EC-SERS progression for 65 μL of 1.0 mg mL^{-1} cortisol deposited on the fabric chip electrode. The spectra were acquired at 785 nm excitation for 30 seconds at a laser power of 42.6 mW.	46
Figure 25. (a) Cathodic (b) Anodic EC-SERS progression for 75 μL of 1.0 mg mL^{-1} cortisol deposited on the fabric chip electrode. The spectra were acquired at 785 nm excitation for 30 seconds at a laser power of 42.6 mW.	47
Figure 26. (a) Cathodic (b) Anodic EC-SERS progression for 100 μL of 1.0 mg mL^{-1} cortisol deposited on the fabric chip electrode. The spectra were acquired at 785 nm excitation for 15 seconds at a laser power of 29.3 mW.	48
Figure 27. Comparison of EC-SERS progression at -0.7V Ag/AgCl for 30, 50, 65, 75 and 100 μg of 1.0 mg mL^{-1} cortisol deposited on the fabric chip electrode. The spectra were acquired at 785 nm excitation for 30 seconds at a laser power of 42.6 mW.	50
Figure 28. Linear trendline in peak intensity for peaks (a)1604 cm^{-1} (b)1328 cm^{-1} (c)1251 cm^{-1} for 50, 65 and 75 μg of 1.0 mg mL^{-1} cortisol.	51

LIST OF ABBREVIATIONS

ACTH	Adrenocorticotropic Releasing Hormone
Ag	Silver
AgCl	Silver Chloride
AgNPs	Silver Nanoparticles
CE	Counter Electrode
CE-IA	Capillary Electrophoresis-Based Immunoassay
CLIA	Chemiluminescence Immunoassay
cm	Centimeter
CRH	Corticotrophin-Releasing Hormone
DHEA	Dehydroepiandrosterone
DSM-5	Diagnostic And Statistical Manual Of Mental Disorders-5
EC-SERS	Electrochemical Surface Enhanced Raman Spectroscopy
ELISA	Enzyme-Linked Immunosorbent Assay
FWHM	Full-Width Half Maximum
GC-MS	Gas Chromatography-Mass Spectrometry
HCG	Human Chorionic Gonadotropin
HPLC-MS/MS	High-Performance Liquid Chromatography-Tandem Mass Spectrometry
KCl	Potassium Chloride
LOD	Limit Of Detection
LSPR	Localized Surface Plasmon Resonance
mL	Millilitre
mm	Millimeter
mW	Milli Watt
NaF	Sodium Fluoride
nm	Nano Meter

nM	Nanomolar
OCP	Open Circuit Potential
p-ATP	Para Amino Thiophenol
POC	Point Of Care
PSA	Prostate Specific Antigen
PTSD	Post-Traumatic Stress Disorder
RE	Reference Electrode
RIA	Radio Immunoassay
SEM	Scanning Electron Microscopy
SERS	Surface Enhanced Raman Spectroscopy
SPE	Screen Printed Electrode
UV-vis	Ultraviolet Visible Spectroscopy
WE	Working Electrode
μ L	Microlitre

1 INTRODUCTION

1.1 Post-Traumatic Stress Disorder (PTSD) and its Causes and Symptoms

Post-traumatic stress disorder (PTSD) is a psychiatric disorder that develops in individuals who have experienced or witnessed life-threatening traumatic or distressing events (Gaskell 2005). Experiencing prolonged stress can lead to development of PTSD in individuals. The diagnosis of PTSD in individuals can be challenging as its symptoms can be confused with those of depression, anxiety, obsessive-compulsive disorder (OCD), etc. According to a survey conducted by the National Centre for PTSD, it has been found that 7 out of 100 Canadians experience PTSD (Van Ameringen et al. 2008).

Experiencing prolonged stressful events can cause an imbalance in the neural hormones that leads to experiencing stress (Young 1995). A patient can experience redefining, reliving, acting out, and hyperarousal behavior because of the memory of trauma (Young 1995). This can result in changes in hormone levels, causing prolonged stress which leads to the development of PTSD. Those experiencing PTSD can exhibit symptoms such as insomnia, anxiety, trouble focusing, depression, eating disorders, nightmares, severe emotional distress, irritability, trouble in maintaining relationships, and self-destructive behavior (Van Ameringen et al. 2008). Some everyday activities can trigger the individual, causing them to think of and relive traumatic events. During the hyperarousal, the individual feels threatened and scared. While feeling emotionally numb, the individual may experience amnesia, social detachment, and may struggle to process emotions (Gaskell 2005). The human body has an inbuilt physiological mechanism to respond to stress where it stress regulating hormones such as catecholamines, corticosteroid-glucocorticoids, and mineralocorticoids which are released from the adrenal gland. These steroid hormones are

derived from cholesterol and are produced by the adrenal cortex, adrenal medulla, and gonads (Waller and Sampson 2018).

1.2 Diagnosis and Treatment of PTSD

Early diagnosis of PTSD is challenging. The prevalence rate of PTSD in Canada is 9.2% (Van Ameringen et al. 2008b). There are clinical guideline methods established to diagnose PTSD in individuals (Van Ameringen et al. 2008). The current diagnostic methods involve performing clinical tests and a psychological evaluation by a psychiatrist. The psychiatrist uses the criteria indicated by the Diagnostic and Statistical Manual of Mental Disorders (DSM-5), published by the American Psychiatric Association (Post-traumatic stress disorder 2018). The psychological evaluation involves the patient sharing their symptoms and traumatic events with the psychiatrist. The patient might not feel comfortable in disclosing and sharing all their symptoms and traumatic events which can lead to an inaccurate diagnosis. Clinical testing methods include Radioimmunoassay (RIA), Enzyme-Linked Immunosorbent Assay (ELISA), Chemiluminescence Immunoassay (CLIA), Capillary Electrophoresis-Based Immunoassay (CE-IA), Gas Chromatography-Mass Spectrometry (GC-MS), and High-Performance Liquid Chromatography-Tandem Mass Spectrometry (HPLC-MS/MS) (Moore and Sharma 2020). These techniques require extensive sample preparation, longer analysis time, the sample may deteriorate over time, and they are expensive and typically located at major hospitals. Newer technologies including wearable sensors may overcome these challenges, especially if they offer advantages including cost-efficiency, rapid analysis time, and ease-of-use.

Treatment of PTSD typically involves a continuous approach towards cognitive behavior therapy, counseling, medications, re-evaluating traumatic symptoms continuously, and recording

symptom severity. Studies have shown that a prolonged time after the traumatic event does not help to decrease the severity of symptoms experienced by the patient (Gaskell 2005). Early diagnosis of PTSD can help with intervention and prognosis, as this may help to recognize stress at an initial stage. Providing appropriate treatment at an early stage will prevent an individual from experiencing prolonged stress.

1.3 Biomarkers for PTSD

A biomarker is a biological marker, a biological entity that provides medical information regarding the medical state of an individual. Examples of biomarkers include ions, small molecules, lipids and proteins. A biomarker should be quantifiable and should be able to help diagnose and monitor a disease state (Strimbu and Tavel 2010). Biomarkers are used for assessing and diagnosing diseases (Schmidt et al. 2013). Early detection of biomarkers in patients will help in initiating treatment during the same clinical visit and will increase treatment efficacy. Biomarkers can be used for the early diagnosis of disease, such as the detection of prostate specific antigen (PSA) for early detection of prostate cancer (Jakobsen et al. 2016). A biomarker should indicate the physiological parameter of the molecule to understand the relation between clinical diagnosis and physiological molecules (Strimbu and Tavel 2010). Biomarkers can be used as a chemical analyte on wearable sensors for both qualitative and quantitative detection. For example, the blood glucose meter measures the concentration of glucose (a biomarker) in the blood of diabetic patients, allowing these individuals to direct their own care in their home environment.

Post-traumatic stress disorder has distinctive neuroendocrine, hormonal, and immunological biomarkers. Some of the known biomarkers include norepinephrine, peripheral α 2-adrenergic receptors, catecholamines, serotonin, cortisol, allopregnanolone, testosterone, and

dehydroepiandrosterone (Michopoulos et al. 2015). The concentration of these biomarkers varies in PTSD patients. Norepinephrine, catecholamines and dehydroepiandrosterone have higher levels in PTSD patients whereas peripheral α 2-adrenergic receptors, serotonin, allopregnanolone and testosterone shows decreased levels in PTSD patients (Michopoulos et al. 2015).

Some of the other immunological biomarkers for PTSD such as interleukin-6, interleukin-1b, interleukin-2, C-reactive protein, nuclear factor-kB, and tumor necrosis factor-a shows an increased level (Michopoulos et al. 2015). Some of the other neuroendocrine biomarkers such as insulin and ghrelin show increased level whereas endocannabinoids, estradiol, glucocorticoid shows decreased or attenuated levels due to negative feedback (Michopoulos et al. 2015). This experimental research focuses on using cortisol as a biomarker for the early diagnosis of PTSD using wearable sensors.

1.3.1 Cortisol

Cortisol is a glucocorticoid stress hormone and a derivative of cholesterol which is produced by the adrenal cortex. When the body experiences stress as a stimulus, the hypothalamus in the brain releases Corticotrophin-Releasing Hormone (CRH). CRH stimulates corticotrophin cells in the anterior pituitary gland to release Adrenocorticotrophic Releasing Hormone (ACTH) (Thau et al. 2021). ACTH targets the adrenal cortex gland to release glucocorticoids and mineralocorticoids. The half-life of cortisol is 66 minutes (McKay and Cidlowski 2003). Even a small release of cortisol in the body will have a long-lasting effect until it is metabolized. The release of cortisol leads to an increase in blood glucose and suppression of the immune system. Prolonged release of cortisol under exposure to continuous long-term stress causes negative feedback which leads to a decrease in cortisol levels in PTSD patients.

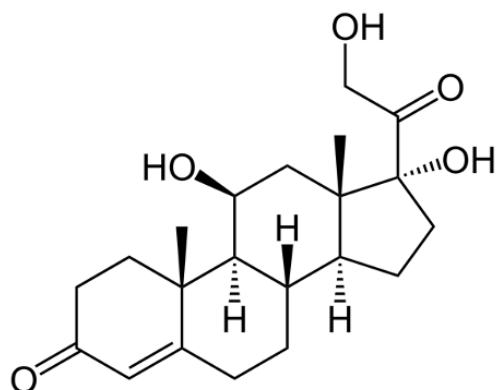


Figure 1. Molecular structure of cortisol hormone, one of the biomarkers used for early diagnosis of PTSD. Chemdraw software was used to draw the molecular structure of cortisol.

The normal range for cortisol levels in a healthy individual is 138-690 nM during the day and 55-386 nM during the evening (Zainol Abidin et al. 2017). As noted above, cortisol concentrations can be measured using clinical methods such as radioimmunoassay (RIA), enzyme-linked immunosorbent assay (ELISA), chemiluminescence immunoassay (CLIA), capillary electrophoresis-based immunoassay (CE-IA), gas chromatography-mass spectrometry (GC-MS), and high-performance liquid chromatography-tandem mass spectrometry (HPLC-MS/MS) (Moore and Sharma 2020). However, these tests are expensive, invasive, and take up to 24 hours to obtain test results. A wearable sensor for direct monitoring of cortisol levels, such as the one being developed for this thesis work, would allow for non-invasive screening tests for early diagnosis of PTSD. Active research is being conducted to find alternative methods for detecting cortisol levels. Moore and Sharma conducted studies on surface-enhanced Raman spectroscopy (SERS) detection of cortisol in both ethanol and a phosphate-buffered saline containing bovine serum albumin (Moore and Sharma 2020). The cortisol concentration was found to be 125-1200 nM and SERS peaks were observed in the range of 200-1800 cm^{-1} (Moore and Sharma 2020).

Similar studies were conducted using gold and silver nanoparticles for detection of cortisol (Apilux et al. 2018). A significant clinical concentration of cortisol in saliva was found to be 0.5-150 ng/mL (Apilux et al. 2018).

1.3.2 Dehydroepiandrosterone

Dehydroepiandrosterone (DHEA) is a steroid hormone that is abundant in the human body. It is also found as its conjugate dehydroepiandrosterone sulphate (DHEAS) (Eberling and Koivisto 1994). Both DHEA and its conjugate DHEAS are biomarkers for PTSD (Yehuda et al. 2006). DHEA is produced by the adrenal cortex (Herbert 2007). DHEA is an important source for producing estrogen and testosterone hormone. The physiological concentration level of DHEA can vary according to the sex and age of the individual. The levels of DHEA in individuals experiencing PTSD are higher than the normal range. Table 1 outlines the normal levels of DHEA.

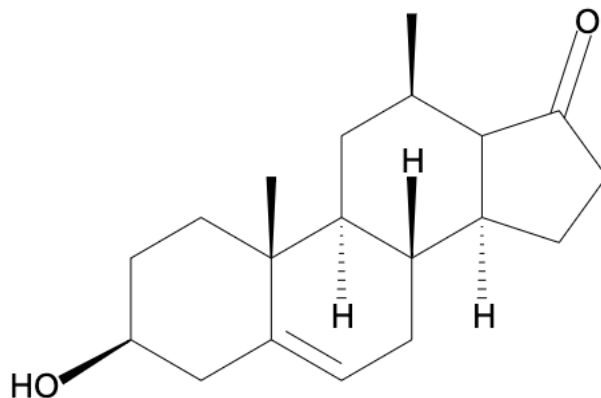


Figure 2. Molecular structure of dehydroepiandrosterone hormone, one of the biomarkers for early diagnosis of PTSD. Chemdraw software was used to draw the molecular structure of dehydroepiandrosterone.

Table 1: Clinical concentrations of dehydroepiandrosterone found in the human body. The DHEA levels vary with the age of an individual (Soldin et al. 2011).

Age	DHEA Levels
Premature	<40 ng/mL*
0-1 day	<11 ng/mL*
2-6 days	<8.7 ng/mL*
7days-1 months	<5.8 ng/mL*
>1-23 months	<2.9 ng/mL*
2-5 years	<2.3 ng/mL
6-10 years	<3.4 ng/mL
11-14 years	<5.0 ng/mL
15-18 years	<6.6 ng/mL
19-30 years	<13 ng/mL
31-40 years	<10 ng/mL
41-50 years	<8.0 ng/mL
51-60 years	<6.0 ng/mL
> or =61 years	<5.0 ng/mL

Individuals experiencing PTSD show higher levels of DHEA (Michopoulos et al. 2015). While this thesis originally sought out to study both cortisol and DHEA, in the end only cortisol detection was evaluated. DHEA analysis will be investigated as part of the follow-on work from this project.

1.4 Electrochemical Surface-Enhanced Raman Spectroscopy (EC-SERS)

Spectroscopy is a technique which involves the interaction of electromagnetic radiation with matter. Raman spectroscopy involves the inelastic scattering of monochromatic light by matter when incident light interacts with the sample. Raman spectroscopy can be used for both qualitative and quantitative analysis of samples. Since Raman scattering is an inelastic scattering process, and only 1 in $\sim 10^6$ photons undergo inelastic scattering, Raman spectroscopy signals are inherently weak. These Raman signals can be intensified with the help of surface-enhanced Raman spectroscopy (SERS). In SERS, the analyte of interest is present on or in very close proximity to a roughened nanoscale metal surface, typically composed of the coinage metals, Au, Ag or Cu. When incident light interacts with these nanoscale metals, the free electrons in the metal particles undergo a collective oscillation, generating a localized surface plasmon resonance (LSPR) (Pelton et al. 2008). This LSPR results in a very intense electromagnetic field at the surface of these nanoparticles, which in turn results in very large enhancements of the Raman signal for the molecules of interest on the metal surface of up to one million-fold or larger. This enhancement of the Raman signal is due to both an electromagnetic mechanism and a chemical mechanism (Sharma et al. 2012). This Raman signal enhancement is particularly evident for particles with sharp edges and/or tips as well as very small (<1 nm) interparticle junctions of plasmonic structures referred to as hotspots. Amplification of radiation signals via application of electric field and dielectric medium allows electromagnetic enhancement (Sonntag et al. 2014). The chemical enhancement occurs due to charge transfer taking place between the adsorbate and the metal surface and vice versa (Sonntag et al. 2014).

Nanostructured metal films and metal nanoparticles play an important role in SERS. Nanoparticles can be prepared either via a top-down mechanism or a bottom-up mechanism

(Pelton et al. 2008). In a top-down technique, larger metal particles are broken down into smaller nanoparticles via mechanical and chemical approaches such as milling, grinding, evaporation, and sputtering. In bottom-up mechanisms, individual atoms or ions are used to make the nanoparticles. Bottom-up is the most common technique used to make nanoparticles as it allows for easier fabrication of nanoparticles.

This study aims to synthesize silver nanoparticles using the bottom-up approach. Silver nitrate, sodium citrate, and sodium borohydride are used as reagents to prepare silver nanoparticles. Silver nitrate is the source for silver, sodium borohydride acts as a reducing agent and sodium citrate is used as both a reducing agent and a capping agent. The capping agent prevents overgrowth and aggregation of the nanoparticles during their synthesis. Ideally, metal nanoparticles used for SERS should have a homogeneous shape, size, and structure. These nanoparticles should be distributed equally in a uniform manner to produce the best SERS enhancement (Pelton et al. 2008). Moreover, these nanoparticles should be biocompatible, cost-efficient, stable over the long term, and resistant to environmental factors such as air, water, and humidity to provide ideal SERS enhancement (Pelton et al. 2008). The plasmonic properties of nanoparticles can be analyzed using ultraviolet-visible spectroscopy to measure the extinction of the particles and scanning electron microscopy (SEM) to measure the nanoparticle size and shape.

Although SERS is sensitive, it has a limitation of being unable to provide strong signals for all molecules, particularly when these molecules are not very close to the metal surface (i.e. not within 1 nm). This challenge can often be overcome using Electrochemical SERS (EC-SERS). In electrochemical SERS, the SERS substrate also functions as the working electrode in a typical three-electrode set-up, and a potentiostat is used to apply a voltage to this electrode. On applying voltage, the surface charge can be manipulated, and the analyte molecules come closer to the

surface, enhancing the SERS signal dramatically (Bindesri et al. 2018). In general, EC-SERS is cost-efficient, sensitive, and biocompatible. Using EC-SERS for analysis of biological samples is ideal as most biological samples are analyzed in an aqueous environment. Since water is a weak scatterer of light it poses little interference during analysis, as compared to infrared spectroscopy, where water is a strong absorber of infrared light and must be corrected for (Marques et al. 2011).

1.5 Point-of-Care Diagnostics

A lack of instruments and technology to diagnose diseases early is leading to an increase in death (Sharma et al. 2015). Currently used instruments are expensive, require long assay times, and are unable to provide quick results in a limited time. Laboratory-based tests require lab instruments, multiple steps, complicated sample handling, and well-trained technicians. To overcome these challenges, point-of-care (POC) diagnostics offer rapid and accessible testing that will enhance disease diagnoses, especially during the first clinical visit (Sharma et al. 2015). POC diagnostics deals with the development of cost and time-efficient devices in the healthcare field to diagnose diseases rapidly and initiate treatment in a timely manner.

POC diagnostics can provide access to clinical diagnostic tests and quality screening techniques to provide worldwide healthcare (Sharma et al. 2015). POC diagnostics are portable, time efficient and generally reliable. Optical, chemical, and physical POC diagnostics are easy to use, non-laboratory based, cost-efficient, reproducible, biocompatible with body fluids, and applicable for chip measurement (Xu et al. 2019). Glucose test strips, pregnancy tests and fit bits are examples of point of care diagnostics. Glucose strips are used for the diagnosis of diabetes at home. These strips detect the blood sugar level when a drop of blood is deposited on the strip. Fitness bands are capable of detecting an individuals heart rate, heartbeats per minute, the number

of calories burned, and the oxygen level in the body. Store bought pregnancy test strips detect the human chorionic gonadotropin (HCG) hormone in urine.

Apart from the advantages, POC devices have certain limitations. Requirement of expensive equipment makes it difficult to develop a cost-efficient way to analyze samples. Other challenges may deal with using body fluids to detect biomarkers and their poor ability to adhere on the sensor. Active research is being conducted on creating portable, cheap, and easy-to-use POC devices. However, there is a lack of POC devices that deal with chemical sensing that can help in the early diagnosis of various diseases through the detection of chemical biomarkers.

1.6 Wearable Sensors

Wearable sensors offer a path towards personalized medicine through the continuous monitoring of various health metrics. These sensors can be worn by the individual and put in contact with the human body to monitor physiological biomarkers (Gao et al. 2016). Flexible plasmonic surface-enhanced Raman spectroscopy wearable sensors are efficient and can detect lower concentration of analytes (Gao et al. 2016). These wearable sensors are biocompatible and easy to use. Currently available wearable sensors are only able to track mostly physical parameters and vitals such as heartbeat, heart rate, and body temperature. Wearable sensors which monitor blood oxygen levels do exist and find routine use in a variety of healthcare settings including in neonatal intensive care units. Recent research studies have demonstrated a smartwatch that can detect stress hormone and cortisol levels in sweat (Wang et al. 2022). A thin adhesive film collects the sweat and attached sensors use aptamers to detect cortisol. When the cortisol attaches to the aptamer, it changes the electric field at a transistor surface.

A lot of focus is being placed on the development of wearable sensors for monitoring the health and lifestyle activities of individuals. An ideal wearable sensor should be smaller in size so

that it can be easily worn by the individual, it should be reusable, flexible, strong, cost-effective, portable, and biocompatible. A perfect point-of-care diagnostic, according to the World Health Organization, must be affordable, sensitive, specific, user-friendly, rapid/robust, equipment-free, and deliverable (ASSURED) (Naseri et al. 2022). Currently available wearable sensors are capable of monitoring physiological and chemical parameters. Besides that, research is being conducted to develop wearable sensors for monitoring symptoms of mental health disorders and their early diagnosis. For example, an ankle-worn wearable sensor was developed that detects ectodermal activity to monitor the autonomous nervous system and sympathetic nervous system for diagnosis of PTSD (Fletcher et al. 2011). Research has also reported the development of a wearable flexible integrated sensing array (FISA) for screening biomarkers in human sweat (Gao et al. 2016). The sensor was able to measure sweat electrolytes (sodium and potassium ions), sweat metabolites (glucose and lactose) as well as skin temperature. Moreover, a wireless garment has been developed to monitor the electrocardiogram (ECG) in babies which are at risk for sudden infant death syndrome (SIDS) (Coosemans et al. 2006). The wireless garment wearable sensor overcomes the challenges faced in the integration and transmission of signals.

1.7 Advancements in Wearable Sensors

With advancements in the textile industry and technology, electronic wearable sensors can be constructed using materials that are durable, washable, deformable, and breathable. Various wearable sensors have been developed to date that offer non-invasive techniques to detect biomarkers. The SERS output of traditional Indian fabric called Zari has also been investigated (Robinson et al. 2015). A fabric chip electrode was created to detect levofloxacin, a commonly prescribed antibiotic in synthetic urine (Bindesri et al. 2018).

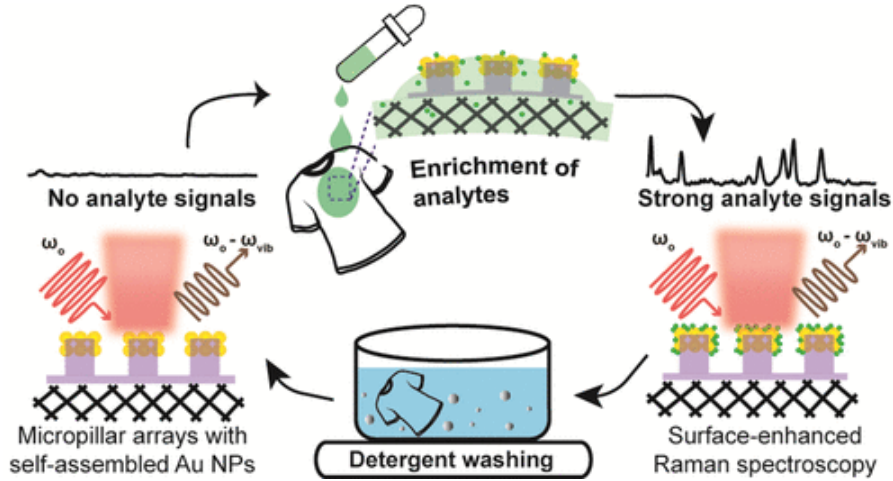


Figure 3. Washable and reusable SERS membrane-based textiles. The reactive ion etching treatment is used to expose the hotspots. SERS textile can be reused by washing of the Au NP wearable sensors in normal detergent with ultrasound sonication and mechanical stirring to remove analyte and contaminants from the hotspot (Garg et al. 2020) (Reproduced with permission).

However, there are certain challenges that arise when designing wearable sensors related to flexibility, launderability, reliable diagnostics, portability, cost-effectiveness, size, and comfort/wearability. Washable and reusable SERS based textile fibers have been developed to overcome some of these challenges (Garg et al. 2020). Figure 3 shows a SERS textile fiber with launderability and reuse ability. The hotspots of the SERS textile fiber can be regenerated via sonification. Surfactants in a detergent bind to R6G molecules, which can be agitated with ultrasound waves, resulting in the R6G molecules being lost, and R6G molecules being removed from hotspots when the temperature and kinetic energy of water molecules rises (Garg et al. 2020). As a result, the SERS textiles can be reused.

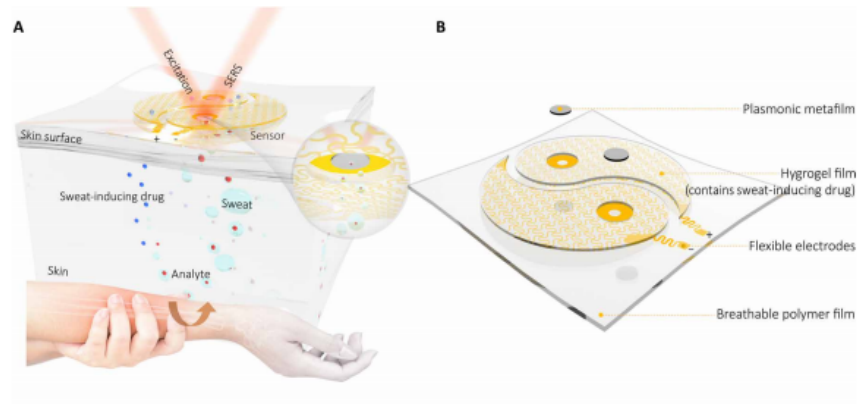


Figure 4. SERS wearable sensor with sweat absorption dermal protective layer. (A) illustrates a schematic representation of the wearable sensor patch used to perform EC-SERS for detecting drug molecules in sweat. (B) illustrates the composition of a wearable sensor patch which is biocompatible with skin (Koh et al. 2021) (Reproduced with permission).

To provide biocompatibility, SERS wearable sensors with a dermal protective layer to detect sweat have been designed (Koh et al. 2021). As shown in Figure 4, a silk fibroin protein layer is used as a basement layer which is coated with silver nanoparticles which is covered by a dermal protective layer that allows the laser to penetrate to the silver nanoparticles (Koh et al. 2021). It is challenging to detect multiple biomarker analytes at the same time. To overcome this challenge, wearable plasmonic sensors with “universal” molecular recognition capability have been developed to diagnose various drugs inside the body (Wang et al.).

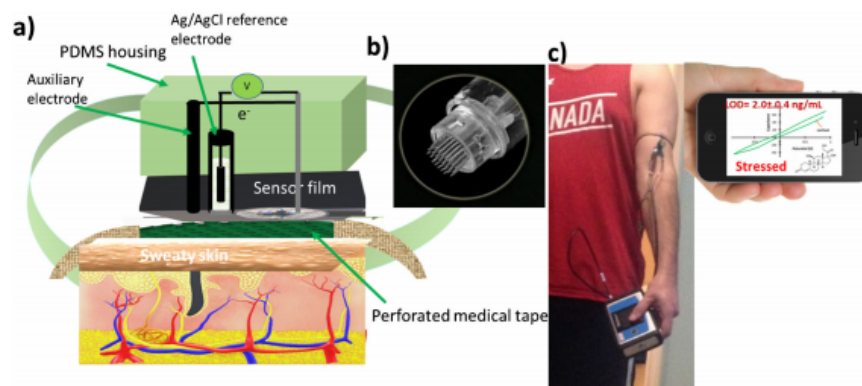


Figure 5. Assembly of a wearable sensor designed to detect cortisol. (A) Illustration of the design of the wearable sensor. (B) The medical tape is perforated using a bayonet microneedle derma pen. (C) describes the working fabric sensor being worn by an individual (Mugo and Alberkant 2020) (Reproduced with permission).

Recent studies have reported on the development of a wearable sensor using medical tape to detect physiological cortisol levels in sweat. 3M double-sided medical tape was perforated with a dermal care Bayonet 36 Pin microneedle pen, and an inset was added (Mugo and Alberkant 2020). When applied to the skin, the medical tape works as a thermal barrier, causing perspiration. On the perforated portion of the medical tape, the sensor was annealed (Mugo and Alberkant 2020). The sensor was placed into touch with the (polydimethylsiloxane) PDMS molded cover plate containing the reference electrode (Ag/AgCl), a platinum counter electrode, and platinum contact for the sensor, which is strapped with a band on the arm of an individual (Mugo and Alberkant 2020). A wireless Palmsens potentiostat was used to probe the embedded sensor, and the results were displayed on the smartphone. The sensor successfully detected a 10–66 ng/mL dynamic range of cortisol (Mugo and Alberkant 2020).

1.8 Fabric Electrodes

Chemical sensors are gaining a dominating role in clinical diagnosis to monitor chemical and physiological information such as heart rate, blood pressure, body temperature, oxygen concentration, and calories. A biosensor should be soft, flexible, reusable, adhesive, strong, and

biocompatible with the human skin. Zari fabric derived from silk which is fibrous textile that has high tensile strength, low inflammability, and good biodegradability to be used as a SERS substrate (Robinson et al. 2015). In this work, Zari fabric was used as a substrate to create a fabric chip. hnn

1.9 Study Objective

This research is focused on the development of an Electrochemical Surface Enhance Raman Spectroscopy (EC-SERS) wearable fabric sensor for early diagnosis of post-traumatic stress disorder using cortisol as the primary biomarker of interest. In particular, optimization of a three-electrode fabric-based EC-SERS sensor was demonstrated for the detection of both para-aminothiophenol as an initial probe molecule for proof-of-concept work followed by cortisol. This research hypothesizes that it will be possible to develop an EC-SERS-based fabric sensor which can detect cortisol at clinically relevant concentrations.

The objectives of this research were:

1. Demonstrate the synthesis of silver nanoparticles using a bottom-up approach. The silver nanoparticles should have homogeneous shape, size and structure.
2. To construct and characterize a functional fabric-based SERS-active electrochemical sensor that will be able to qualitatively and quantitatively measure cortisol as a marker for early PTSD detection.
3. To perform electrochemical SERS on fully functional fabric electrodes to detect various concentrations of cortisol for proof-of-concept validation.

2 MATERIAL AND METHODS

2.1 Reagents and Solutions

Sodium citrate (99%), citric acid ($\geq 99\%$), sodium fluoride (99%), *para*-aminothiophenol (*p*-ATP, 97%) and a cortisol analytical standard (1.0 mg/mL in methanol) were purchased from Sigma-Aldrich (St. Louis, MO). Sodium borohydride (NaBH_4 , 99%) was purchased from Fluka Analytical (Sleeze, Germany). Silver nitrate ($\geq 99.9995\%$) was purchased from Alfa Aesar (Wardhill, MA, USA). Potassium chloride was purchased from Chimiques ACP Chemicals (Saint-Leonard, QC Canada). Blend fabric (37% silk, 35% hemp, 28% organic cotton) was purchased from Pickering International, Inc. (San Francisco, USA). 7565-M Silver Conductor Ink (100 gm) and 6720 Carbon Conductor Paint (200 gm) were purchased from Applied Technologies, Inc. (PA, USA). All glassware was soaked in sulfuric acid for a period of 24 hours, rinsed with Millipore water ($\geq 18.2 \text{ M}\Omega \text{ cm}$) and dried with argon gas (argon gas 9.999%, Praxair Canada Inc., Ontario, Canada) prior to use. Transparent nail polish was used to treat the fabric electrodes (14.7 mL, Sally Hansen).

2.2 Instrumentation

All spectroelectrochemical measurements were conducted using screen-printed electrodes and fabric electrodes. Screen-printed electrodes (SPE) with a rectangular 4x5 mm working carbon electrode surface, a carbon counter electrode and a Ag/AgCl reference electrode were purchased from Pine Research Instrumentation (Durham, NC, U.S.A.). The SPE was placed into a glass vial containing supporting electrolyte and was connected to a potentiostat with cables and coupled to an Advantage 785 Raman spectrometer (DeltaNu Raman spectrometer, Intevac Photonics, Santa Clara). A portable USB Wavenow potentiostat/galvanostat (Durham, NC, U.S.A.), purchased from Pine Research Instrumentation was used for conducting electrochemical measurements. Pine

Research Instrumentation also produced the electrochemical software, Aftermath Data Organizer (version 1.2.4843). Aftermath Data Organizer was used to conduct open circuit potential (OCP) measurements and apply potentials for electrochemical surface enhanced Raman spectroscopy (EC-SERS) measurements. The Aftermath Data Organizer was also used to perform cyclic voltammetry on screen printed and fabric electrodes.

The Raman spectrometer was connected to a laptop computer and signal processing was conducted using NuSpec software. The Raman spectrometer is equipped with a 785 nm diode laser. The EC-SERS spectra were collected using laser powers and acquisition times typically between 22.3–55.9 mW and 30–60 s, respectively. The resolution of the spectrometer was 4 cm^{-1} . UV-vis spectroscopy and scanning electron microscopy (SEM) were used for characterization of the silver nanoparticles. The SEM was a TESCAN MIRA 3 LMU Variable Pressure Schottky Field Emission Scanning Electron Microscope was used for characterization.

2.3 Synthesis of Silver Nanoparticles

The synthetic strategy for producing silver nanoparticles has been previously reported (Zhao et al. 2015). Briefly, in an aluminum foil-wrapped three neck round flat-bottomed flask, 1.00 mL of 0.1 M AgNO_3 , 3.4 mL of 0.17 M sodium citrate, 0.6 mL of 0.17 M citric acid, and 95 mL of water were added. The mixture was stirred at 400 rpm. 0.2 mL of 0.1 mM NaBH_4 was added to the mixture and was then put under reflux for 1 hour 20 minutes at 225°C and magnetic rotation at 400 rpm. The colloidal suspension formed was allowed to cool down for 1 hour. 1.5 mL of silver nanoparticle colloidal suspension was transferred into 48 2 mL size Eppendorf tubes (16x3 tubes) and centrifuged for 20 minutes at 8000 rotations per minute using a microcentrifuge (MC-24 touch, Item C2417). The supernatant was removed via micro pipetting, and the colloidal suspension from 16 tubes was transferred into one Eppendorf tube. The three Eppendorf tubes with silver

nanoparticle colloid were centrifuged again for 20 minutes at 8000 rotations per minute. The supernatant was removed, and silver nanoparticle paste was collected. To prepare an adequate final volume of 50 μL of silver nanoparticle paste an appropriate amount of Millipore water was added to the collected silver nanoparticles.

2.4 Preparation of EC-SERS Sensors

2.4.1 Preparation of Screen-Printed Electrodes

A 1-10 μL micropipette was used to perform 3 depositions of 5 μL silver nanoparticle paste onto the rectangular surface area of the working electrode of the carbon screen-printed electrode. The silver nanoparticle deposition was allowed to dry at room temperature for 15 to 25 minutes. The electrode was chloride-treated in a glass vial with 0.5 M KCl for 30 minutes to replace the adsorbed citrate ions as this would eliminate any interfering SERS signals from the citrate anions. After chloride treatment, the electrode was washed with Millipore water for 30 seconds to remove residual chloride. 50 μL of the cortisol standard (1mg/mL methanol, Sigma Aldrich) was then introduced onto the working electrode with help of a micropipette by adding 5 μL cortisol in 10 intervals. During each interval, 5 μL cortisol was deposited and was allowed to dry for 5 minutes.

2.4.2 Preparation of fabric electrodes

Previous studies in the Brosseau research group have been conducted to determine the optimal fabric for producing fabric-based SERS-active sensors (Alhatab 2017). A piece of blend fabric (37% silk, 35% hemp, 28% organic cotton) was deemed optimal, since it provides sufficient strength while also being absorbent. Follow on studies had developed a protocol for the production of fabric-based EC-SERS substrates (Bindesri et al. 2018). This protocol was used for this thesis work as well and is briefly described here. The fabric was first mercerized by treating it with 0.25

M NaOH for 30 minutes. The dyeability and elasticity of cellulose-based fabrics is improved by the process of mercerization (Bindesri et al. 2018). After 30 minutes, the blend fabric was washed with Millipore water to remove any residual base and was allowed to dry for 30 minutes. As shown in Figure 6, the fabric sensor consists of a reference electrode, a working electrode and a counter electrode. The counter electrode, reference electrode, and working electrode were traced onto the fabric with silver conductive ink using a glass pipette. The fabric chip was allowed to dry in the oven at 90°C for 20 minutes. A first layer of carbon conductive ink was imprinted on the working electrode and counter electrode. The electrode was kept in the oven to dry at 90°C for 10 minutes. The above step was repeated to imprint a second layer of carbon conductive ink on the counter electrode and working electrode. 1 to 2 drops of saturated KCl were deposited on the reference electrode to provide the Ag/AgCl reference electrode. A thin layer of clear nail polish was also applied on the top of the fabric electrode to prevent water from moving to the leads of the fabric chip through capillary action, which could result in short-circuiting of the chip.

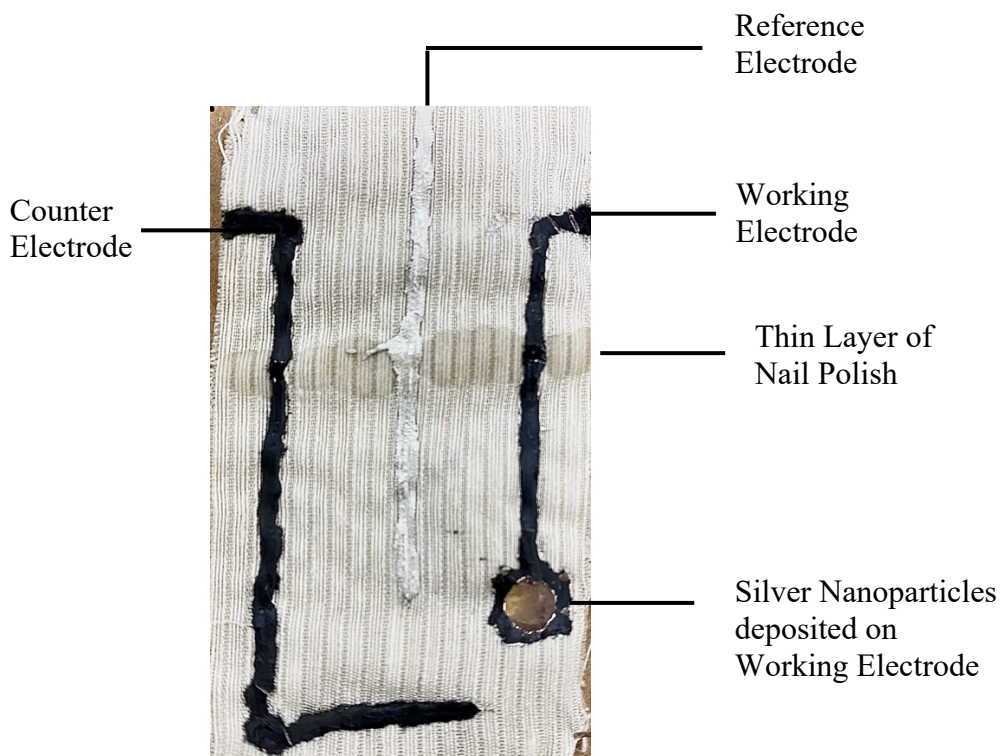


Figure 6. Fabric sensor showing reference, working and counter electrode traced with silver conductive ink and carbon electrode, working electrode traced with carbon inductive ink on top of silver conductive ink.

Three layers of 5 μL silver nanoparticle paste was deposited onto the carbon working electrode on the fabric. To prevent interference from surface-adsorbed citrate which has a strong SERS signal, the working electrode was immersed in 0.5M KCl for 30 minutes and then rinsed with Millipore water for 30 seconds. The fabric electrode was allowed to dry for 25 to 30 minutes. The analyte was introduced by depositing a varying amount of cortisol (30-100 μL) onto the working electrode.

2.5 Electrochemistry

Characterization of fabricated screen-printed electrodes (SPE) and fabric electrodes was conducted by performing cyclic voltammetry (CV). This technique was chosen as it is fast and provides a quick “snap shot” of the electrochemical performance of the chip. A 50 mL supporting

electrolyte solution of 0.1M NaF was prepared and purged with argon gas for 20 minutes to remove dissolved oxygen. The SPE was immersed in 0.1M NaF solution in a glass vial, while the fabric electrodes were soaked in purged 0.1M NaF prior to measurement.

The SPE was connected to a potentiostat through a USB cable. Aftermath Data Organizer was used to conduct open circuit potential (OCP) and cyclic voltammetry (CV) measurements. OCP was conducted for a time interval of 20 seconds to evaluate if the cables and setup were connected properly and to test if the electrode chip was functioning properly. CV measurements were conducted between 0.0 V and -1.0 V with a sweep rate of 50 mV s⁻¹.

2.6 EC-SERS Studies

2.6.1 EC-SERS studies with Cortisol on Fabric Sensor

EC-SERS cortisol studies were conducted using 50 μ L of 1mg/mL cortisol in methanol. Before depositing cortisol on the fabric sensor, an “In Air” Raman spectrum was collected for the silver nanoparticle working electrode surface. This “In Air” spectrum is important as it represents the signal achievable in the absence of an applied potential (essentially a non-electrochemical SERS signal). Typically, the main spectral feature is a large Ag-Cl stretching vibration around 230 cm⁻¹ which originates from the AgCl film on the surface. The Ag-Cl peak indicates the fabric sensor is good to be used for depositing cortisol and performing EC-SERS. Next, 50 μ L of 1 mg/mL cortisol was deposited using a micropipette in 10 x 5 μ L aliquots. During each deposition, 5 μ L cortisol was deposited and was allowed to dry for 5 minutes. As shown in Figure 7, the fabric sensor was placed in a petri dish and electrodes were connected to potentiostat (Pine Research Instrumentation portable USB Wavenow potentiostat /galvanostat (Durham, NC, USA)). The

fabric sensor was placed under the right angle optics attachment of the Raman spectrometer (Advantage 785 Raman spectrometer, Intevac Photonics, Santa Clara).

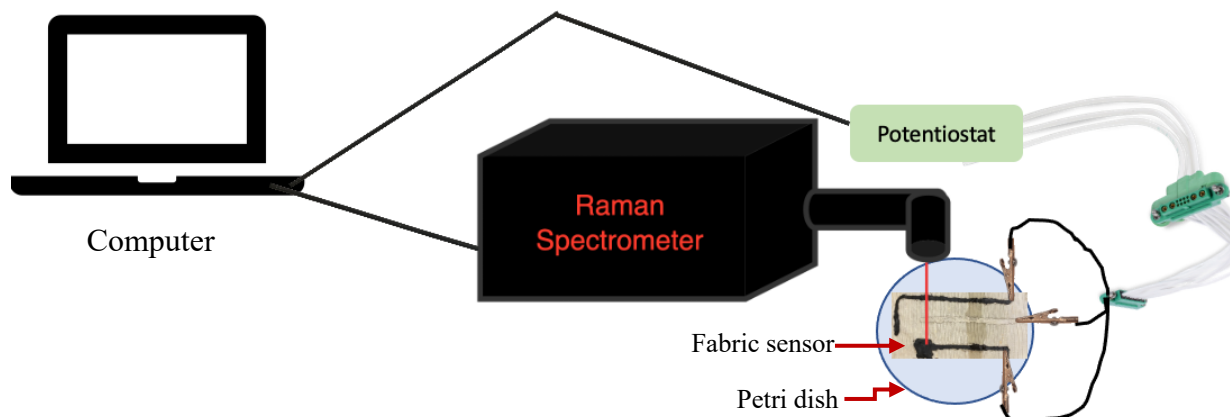


Figure 7. EC-SERS set up for fabric electrode drawn using chemix software. The fabric electrode is connected to the potentiostat through cables. The Raman spectrometer is connected to a computer and the sample is analyzed using a 180° backscattering configuration.

The Raman spectrometer has a resolution of 5 cm^{-1} . An air-cooled CCD detector was equipped with the benchtop Raman spectrometer. NuSpec software was used to conduct Raman spectroscopy and Aftermath Data Organizer was used to apply potential to the working electrode. The laser was turned on and focused on the working electrode at a focal length of 1.6 cm. The excitation wavelength was 785 nm and the laser power ranged from 22.3–55.9 mW and an acquisition time of 30 seconds was used to acquire the EC-SERS measurements. NaF electrolyte was purged with argon gas (99.999%, Praxair Canada Inc., Ontario, Canada). “In Air” Raman spectrum was collected. The electrode chip was immersed in purged 0.1 M NaF supporting electrolyte. The open circuit potential (OCP) signal was collected and then the potential was stepped in the cathodic direction from 0.0 V to -1.0 V in 100.0 mV increments and the SERS spectrum was collected at each step. Next, the potential was stepped in the anodic direction from

-1.0 V to 0.0 V in 100.0 mV increments and again the SERS spectrum was collected at each potential. To prevent any interference from external light sources, EC-SERS spectra were collected in a darkened room. With the help of Origin 9.0 software (OriginLab Corporation, Northampton, MA, USA), the collected data was analyzed.

3 RESULTS AND DISCUSSION

3.1 Characterization of Silver Nanoparticles (AgNPs)

3.1.1 UV-vis Spectroscopy of AgNPs

UV-vis spectroscopy was used for the characterization of the colloidal silver nanoparticles. In general, the position of the extinction band (also referred to as the localized surface plasmon resonance (LSPR) band) is reflective of the average size of the colloidal silver particles, and the full-width half maximum (FWHM) is reflective of the size distribution of the nanoparticles (Kravets et al. 2018). Figure 8 shows the UV-vis extinction spectrum for the silver nanoparticles synthesized in this research project. An LSPR band at 394 nm was observed in the UV-vis spectrum with a FWHM of 54 nm. This result indicates that the colloidal AgNPs synthesized in this project are of an appropriate size (~30 nm diameter, in comparison to prior work) and are nearly monodisperse in terms of size and shape, as reflected in the relatively low FWHM. This preliminary finding was next confirmed using scanning electron microscopy.

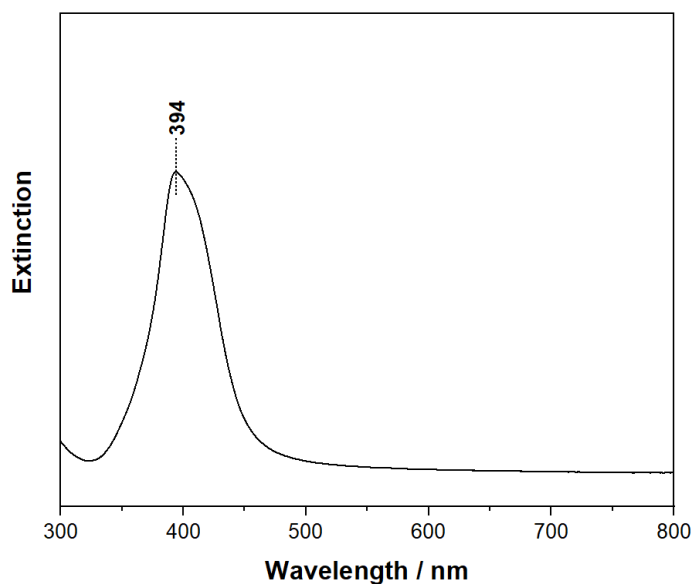


Figure 8. UV-vis extinction spectroscopy of the colloidal silver nanoparticles used in this research.

3.1.2 Scanning Electron Microscopy (SEM)

Scanning electron microscopy (SEM) was also used for the characterization of the AgNPs nanoparticles. Figure 9 shows the SEM image for the AgNPs deposited onto a silicon wafer at 200kx magnification. Using ImageJ software (National Institutes of Health, Maryland, USA), it was found that the diameter of these silver nanoparticles was approximately $27.5 \text{ nm} \pm 4.0 \text{ nm}$. Table A1 (Appendix) shows the reported diameter of 20 nanoparticles along with the calculated mean and standard deviation.

This result indicates that the AgNPs synthesized in this work are of the correct size for efficient SERS activity, and in addition they are uniform in size and shape which should lead to a uniform SERS signal, which is particularly important for quantitative SERS analysis.

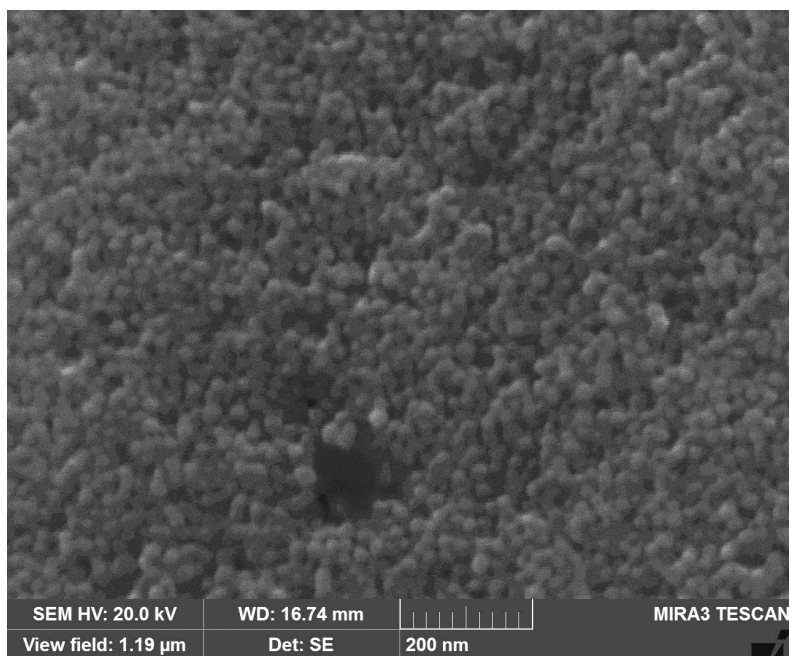


Figure 9. SEM image of silver nanoparticles observed at a magnification of 200kx.

3.2 Fabrication and Characterization of EC-SERS sensors

3.2.1 Fabrication and Characterization of the Fabric Chip Electrode

A blend fabric (37% silk, 35% hemp, 28% organic cotton) was used to fabricate a functional fabric sensor. The fabric was mercerized before deposition of carbon conductive ink. Mercerization involves treating the fabric with an alkali, and helps to improve the smoothness of fabric, increases dye affinity and enhances fabric strength. (Bindesri et al. 2018). Mercerization increases the dyeability which helps the ink stay intact on the fabric. As shown in Figure 10, the fabric sensor has a working electrode, counter electrode, and reference electrode. Silver conductive ink and carbon ink was painted on the fabric using the tip of a glass pipette. Mercerizing the fabric before application of the conductive ink helps improve the ink's adhesion onto the fabric. All three electrodes have silver conductive ink as the first layer, and a carbon ink layer was painted on top of the silver ink for the counter electrode and working electrode. The adherence of silver ink on the fabric after being mercerized allows it to stay intact even after application of voltage. A functional reference electrode is produced by depositing a small volume of saturated KCl onto the silver reference electrode, forming a silver/silver chloride electrode (Ag/AgCl). Having silver conductive ink as the first layer ensures a steady flow of current through the fabric sensor while performing EC-SERS, even if there is a minor break in the carbon ink layer. Moreover, for optimizing the functionality and reproducibility of the fabric sensor, it was important to ensure that all three electrodes had a minimum thickness of 1.5 mm to 2 mm. Having an appropriate design for the sensor allows it to be reproducible. The area of the working electrode where silver nanoparticles are deposited should be approximately 5 mm in length and 5 mm in width. Drop coating silver nanoparticles onto the working electrode can be a bit challenging because they do not spread easily over the carbon ink on fabric and may coagulate or even mix with the carbon ink.

Therefore, it is important to make sure that the underlying carbon ink is completely dry prior to deposition of the silver nanoparticles.

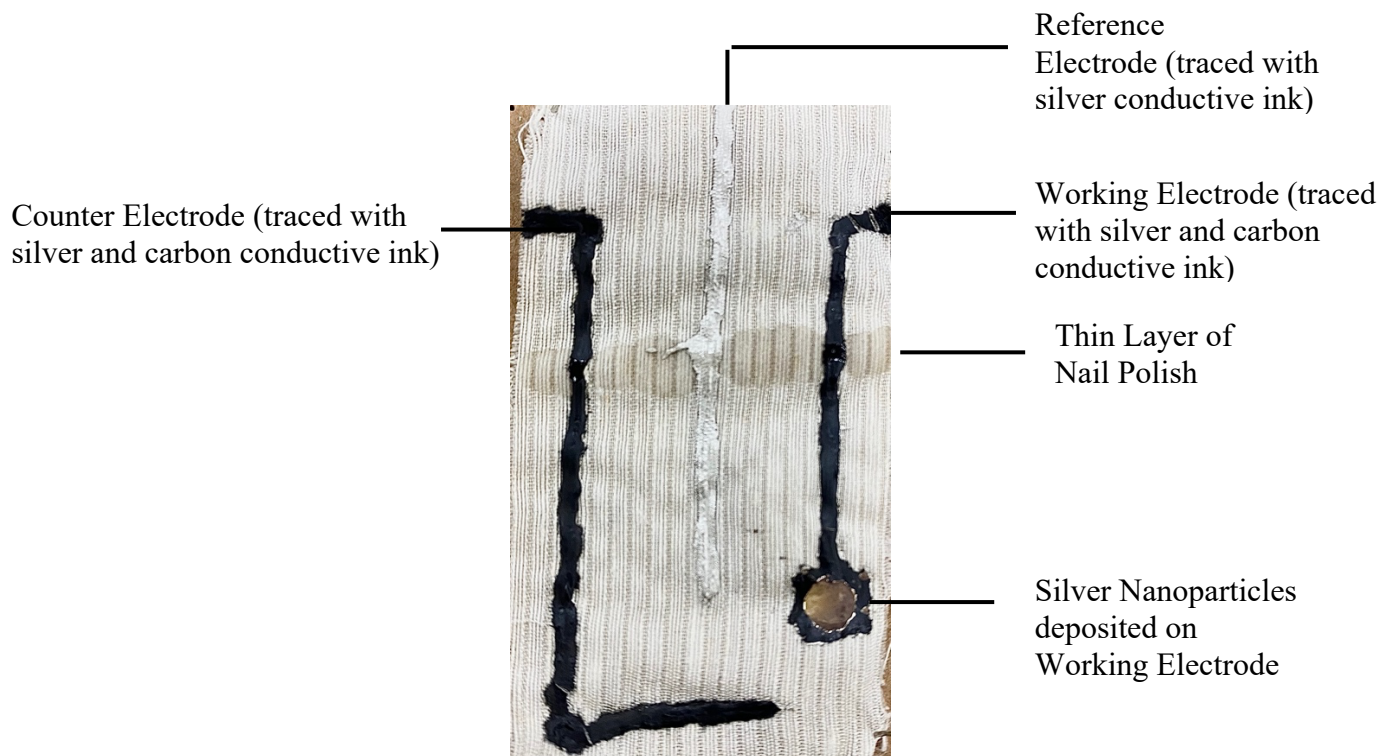


Figure 10. Fabric sensor showing reference, working and counter electrode traced with silver conductive ink and carbon electrode, working electrode traced with carbon conductive ink on top of silver conductive ink.

While performing EC-SERS on the fabric sensor, 0.1 M NaF is used as a supporting electrolyte. When the supporting electrolyte is added to the sensor, it can reach the top layer of the fabric. This can result in short circuiting as it would wet the cables attached to the electrodes. Therefore, applying a single thin layer of nail polish on the fabric sensor can help in preventing the supporting electrolyte from wetting the top of the sensor and prevent short circuiting of the sensor.

para-Aminothiophenol (*p*-ATP) was used as a probe molecule to characterize the functionality of the fabric sensor. *p*-ATP shows an intense EC-SERS signal as it can form a strong

Ag-S bond at the SERS substrate surface resulting in an enhanced SERS signal. Two depositions of 5 μL of a 1.0 mM aqueous solution of *p*-ATP were deposited on the working electrode with the help of a micropipette. The *p*-ATP SERS signal is visible at OCP, and its intensity increases with application of voltage, indicating that the fabric sensor is functional. *p*-ATP shows an intense SERS signal due to its ability to form a strong Ag-S bond and was used in this work as it has been well studied in the literature (Bindesri et al. 2018). Figures 11 and 13 show the cathodic and anodic progression of the *p*-ATP signal on the fabric chip electrode, respectively.

The EC-SERS signal for *p*-ATP was observed to be maximum at -0.9 V for the cathodic progression (Figure 12) and -0.8 V for the anodic progression (Figure 14). These studies indicate that the fabric chip is working as an EC-SERS sensor and should prove useful for the detection of cortisol.

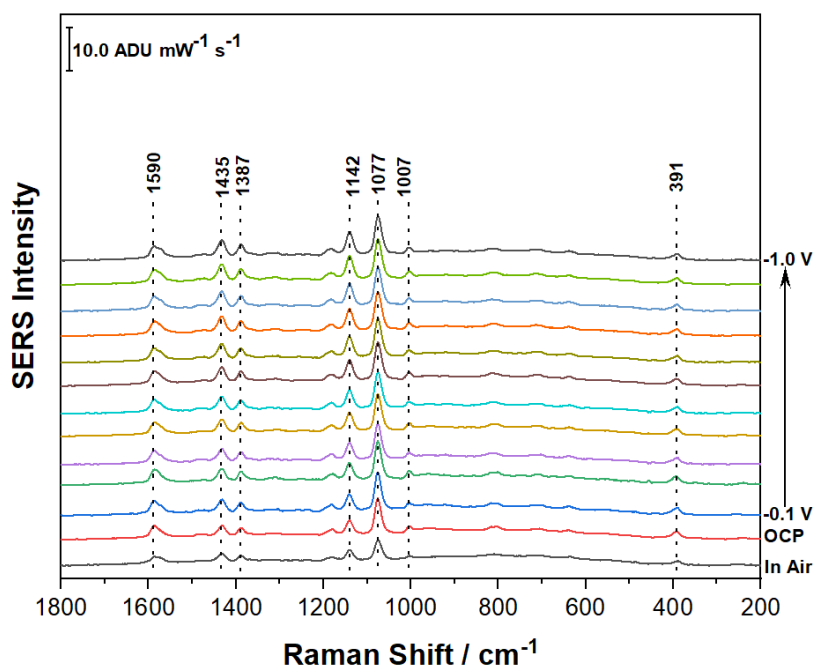


Figure 11. Cathodic EC-SERS progression for 10 μL of 1.0 mM *p*-ATP deposited on the fabric chip electrode. The spectra were acquired at 785 nm excitation for 30 seconds at a laser power of 42.6 mW.

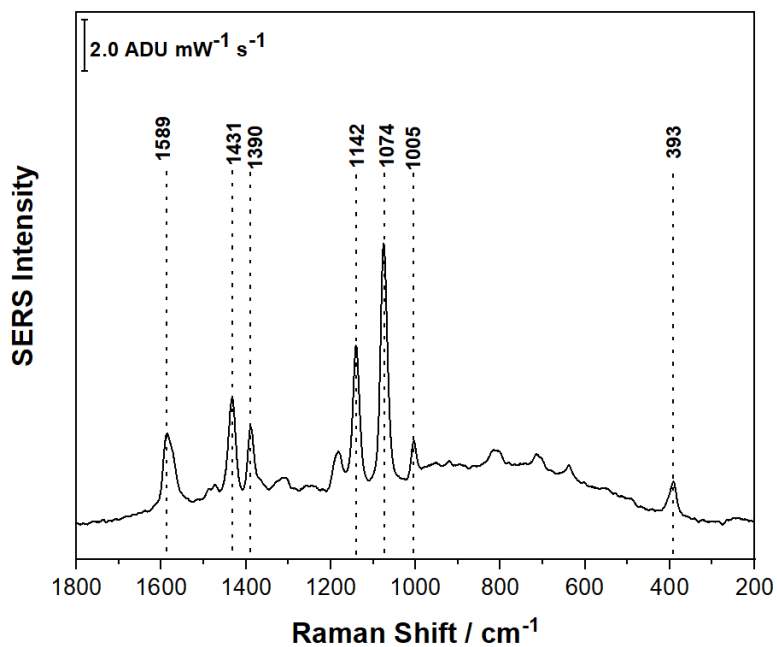


Figure 12. EC-SERS spectrum at -0.9 V vs Ag/AgCl for 10 μ L of 1.0 mM *p*-ATP deposited onto the fabric chip electrode. The spectrum was acquired at 785 nm excitation for 30 seconds at a laser power of 42.6 mW.

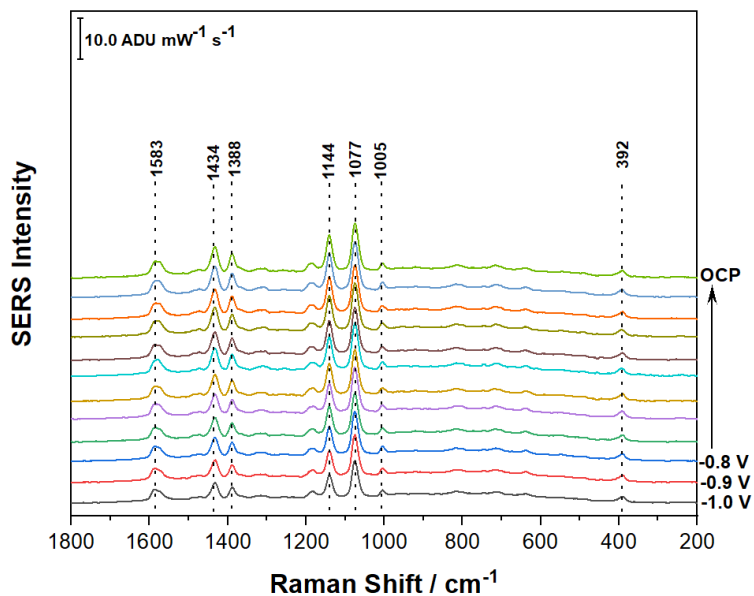


Figure 13. Anodic EC-SERS progression for 10 μ L of 1.0 mM *p*-ATP deposited on the fabric chip electrode. The spectra were acquired at 785 nm excitation for 30 seconds at a laser power of 10.6 mW.

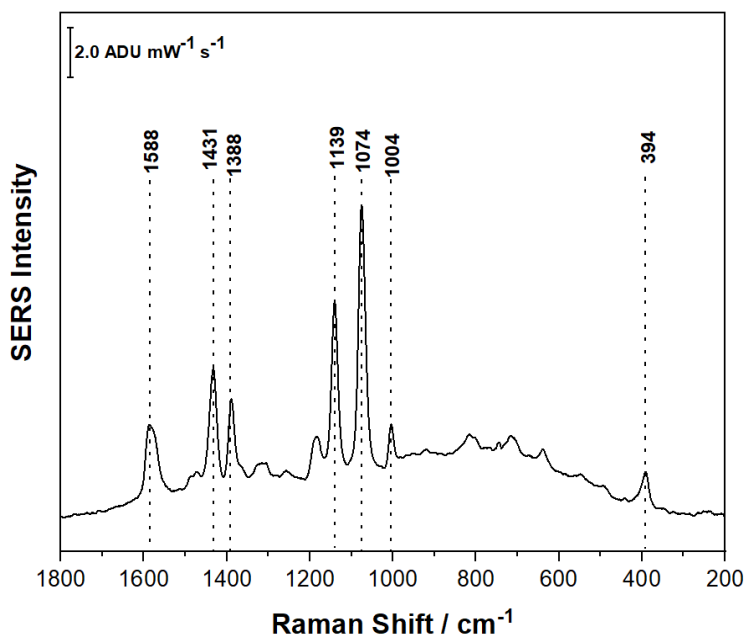


Figure 14. EC-SERS spectrum at -0.8 V vs Ag/AgCl for 10 μ L of 1.0 mM *p*-ATP deposited onto the fabric chip electrode. The spectrum was acquired at 785 nm excitation for 30 seconds at a laser power of 42.6 mW.

3.2.2 Electrochemistry

In order to assess the electrochemical performance of the fabric sensor, cyclic voltammetry (CV) was conducted in 0.1 M NaF. This supporting electrolyte was chosen since the fluoride anion has a weak specific adsorption on silver, and therefore does not contribute to the measured signal. The NaF electrolyte solution was purged with argon gas for 20 minutes to remove dissolved oxygen in order to avoid any interference while performing cyclic voltammetry (CV). In cyclic voltammetry, the electrified interface is modelled as a parallel plate capacitor, and in the absence of a Faradaic contribution to the current, the cyclic voltammogram resembles a rectangle. Figure 15 shows the first and last cycle of the CV for the fabric sensor with 0.1 M NaF as an electrolyte. The CV indeed resembles a rectangle, albeit with a diagonal directionality, a reflection of a resistive component to electron transfer in the system. This is not surprising, as it is expected that current flow will face resistance when moving through this fabric-based system. Since the current

is stable as the potential is cycled, it can be concluded that the fabric chip is functioning as an electrochemical sensor.

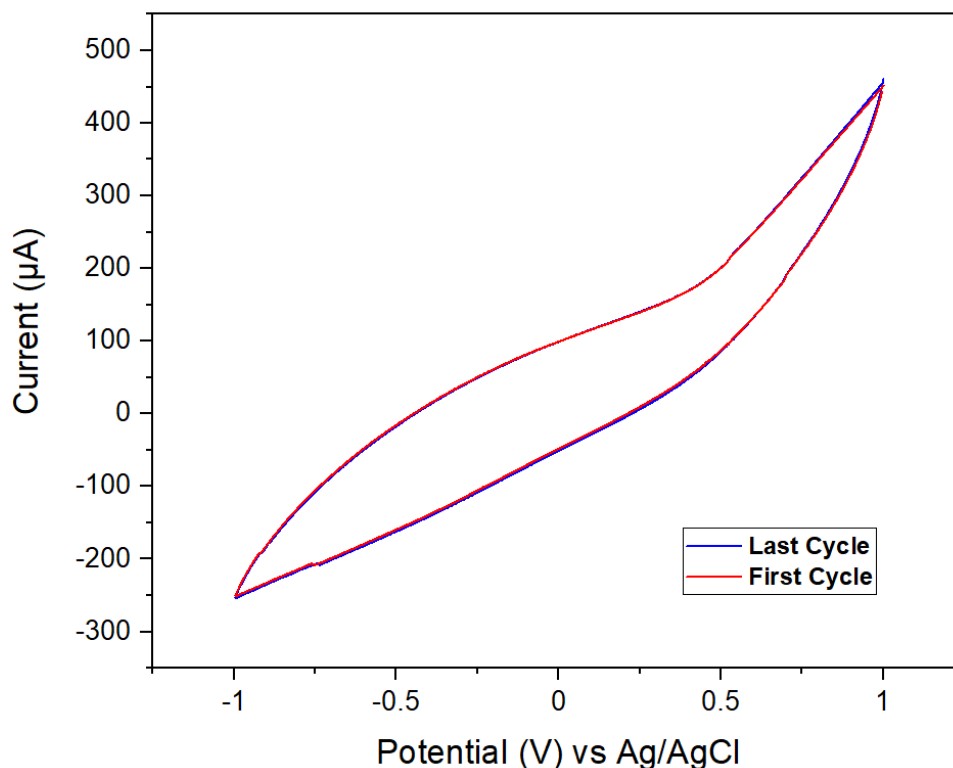


Figure 15. Cyclic voltammetry (CV) plot showing the first and last cycle for the fabric sensor. Supporting electrolyte: 0.1 M NaF, Sweep rate: 50 mV s⁻¹.

3.3 EC-SERS of Cortisol

3.3.1 EC-SERS for cortisol on the fabric sensor

Unlike *p*-ATP, cortisol is a challenging molecule to detect as it does not form strong bonds with silver. Only a few studies have been conducted in the past on SERS of cortisol, and none of these published works use EC-SERS. SERS was used in the past to detect cortisol over the physiologically relevant range (Moore and Sharma 2020). In this work, the authors determined the limit of detection to be 177 nM (Moore and Sharma 2020).

In this thesis work, initial experiments were performed using 30 μL of a 1 mg mL^{-1} cortisol standard deposited onto the working electrode. As shown in Figure 16, the peak intensity was too weak to be detected in air (“in air” spectrum), as well as after the addition of electrolyte but before application of voltage (open circuit potential (OCP) spectrum). As the potential was stepped in the negative direction, a weak signal for cortisol can be observed. The peak observed at 1601 cm^{-1} indicates the carbon-carbon double bond in cortisol, peaks observed in 1000 to 600 cm^{-1} are because of the cholesterol skeleton in cortisol.

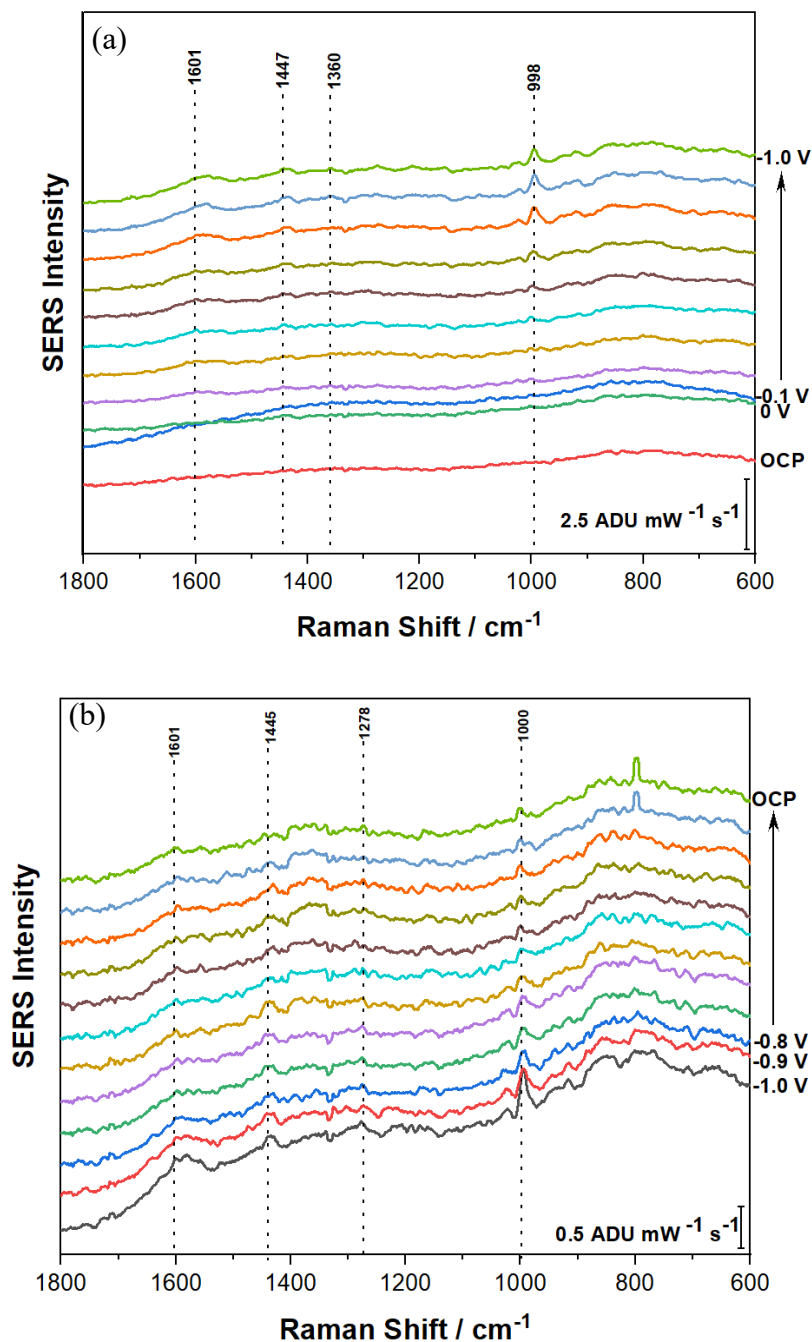


Figure 16. (a) Cathodic (b) Anodic EC-SERS progression for 30 μL of 1.0 mg mL^{-1} cortisol deposited on the fabric chip electrode. The spectra were acquired at 785 nm excitation for 30 seconds at a laser power of 42.6 mW.

Due to the weak signal observed, the amount of deposited cortisol was increased to 50 μL . 10 depositions of 5 μL cortisol was deposited on the working electrode using a micropipette. To prevent transfer of cortisol onto other areas of fabric sensor, it was important to use small volumes

for the deposition. A 50 μL deposition of cortisol resulted in the ability to readily detect cortisol EC-SERS peaks as seen in Figure 17. The intensity of the cortisol peaks increased with an increase in negative applied voltage. To ensure the results obtained are significant and accurate, limit of detection for the signal was calculated. Signal limit of detection (LOD) is the lowest amount of analyte that can be detected with statistical significance. It can help to determine the noise level in the spectrum and to verify the peaks reported. Limit of detection can be calculated by using Equation 1, where σ is the standard deviation of the background spectral noise:

$$\text{LOD} = 3\sigma \quad \text{Equation 1}$$

The signal LOD value calculated for EC-SERS analysis of 50 μL cortisol was 0.45 $\text{ADU mW}^{-1} \text{ s}^{-1}$.

For the reported peaks to be significant, and therefore useful for qualitative analysis, the signal intensity must be greater than this signal LOD. The calculations for the signal LOD determination are shown in the Appendix in Table A2.

All the reported peaks were compared to the limit of detection value. If the difference between the y-value and baseline of THE reported peak is greater or equal to the value of limit of detection, then the reported peak was considered significant. Replicate studies were conducted with 50 μL of 1mg/mL cortisol to show the reproducibility of the sensor's ability to detect cortisol. Appendix Table A3 shows the calculated coefficient of variation for a few selected peaks. The coefficient of variation indicates the percentage error among the peak intensity reported for two trials of 50 μL of 1mg mL^{-1} cortisol. The calculated coefficient of variation is 27.55 %, 52.66 %, 29.63 % and 65.07 % for peaks reported at 1604, 1325, 1251 and 1072 cm^{-1} respectively. The coefficient of variation indicates the dispersion around the mean. Peaks at 1325 and 1072 cm^{-1} have a higher coefficient of variation which indicates these peak intensities are highly variable.

Higher CV values indicates that the data is not accurate and have higher error rate. This may be due to poor reproducibility of fabric sensor.

Once the fabric chip was deemed to be useful for EC-SERS measurements, this thesis research then moved to focus on the detection of cortisol. In past studies, only a few SERS studies on cortisol have been reported, with no EC-SERS studies of cortisol reported to date. Cortisol is a challenging molecule to detect using EC-SERS. This is because of the planar structure of cortisol and its lack of ability to adhere to the silver nanoparticles. These studies have reported using SERS and metal nanoparticles such as gold and silver nanoparticles for the detection of the clinically relevant concentration of cortisol in sweat and serum. A study conducted by TJ Moore was successful in detecting cortisol peaks in the range of 1200 to 1600 cm^{-1} with a limit of detection at 177 nM (Moore and Sharma 2020). To date, there have not been any SERS studies of cortisol reported for fabric-based substrates nor have there been any EC-SERS studies on cortisol, and so this thesis research provides new research in this area.

For proof-of concept studies for this thesis research, a 1 mg mL^{-1} analytical standard of cortisol in methanol was used for these investigations. To start, 30 μL of the 1 mg mL^{-1} cortisol standard was deposited onto the surface of the fabric sensor and EC-SERS measurements in 0.1M supporting electrolyte were conducted. However, the signal intensity for 30 μL of the 1 mg mL^{-1} was weak, as shown above in Figure 16. Therefore, the concentration was increased, and EC-SERS was performed using 50 μL of the 1 mg mL^{-1} . Figure 17 shows the EC-SERS plot for the cathodic progression for 50 μL of 1 mg mL^{-1} cortisol. The “in air” signal represents the SERS signal collected for the deposited cortisol layer without the application of potential. In this case, no SERS signal for the cortisol can be observed. Once the supporting electrolyte is added, the SERS signal is again collected without the application of potential, referred to as the open circuit potential

(OCP) signal. Again, at OCP no signal for the cortisol can be observed. As the potential is stepped in the negative direction, the cortisol signal can be observed starting at ~ -0.4 V and is maximum at -0.7 V (Figure 18). This indicates that as the potential is stepped in the negative direction, the cortisol signal can be observed, likely due to the reductive desorption of chloride ion starting at -0.4 V, which allows cortisol to then access the bare metal surface, resulting in a SERS signal. Upon returning back to OCP in the anodic direction (Figure 19), the SERS signal for cortisol remains strong with a slight weakening in signal as 0.0 V is approached.

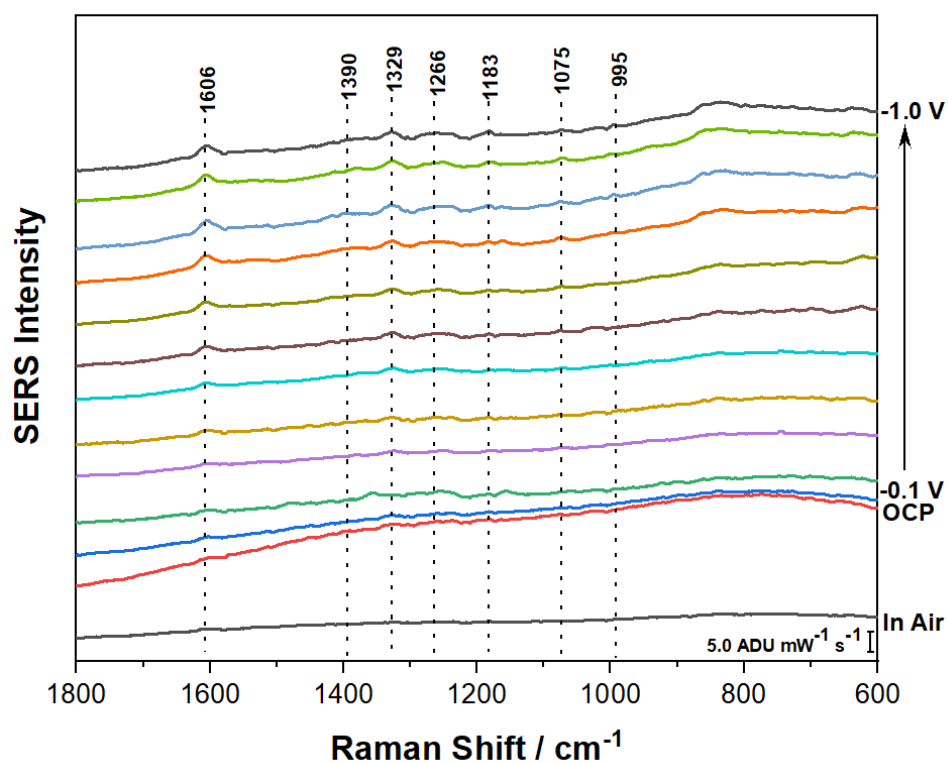


Figure 17. Cathodic EC-SERS progression for $50 \mu\text{L}$ of 1.0 mg mL^{-1} cortisol deposited on the fabric chip electrode. The spectra were acquired at 785 nm excitation for 30 seconds at a laser power of 42.6 mW .

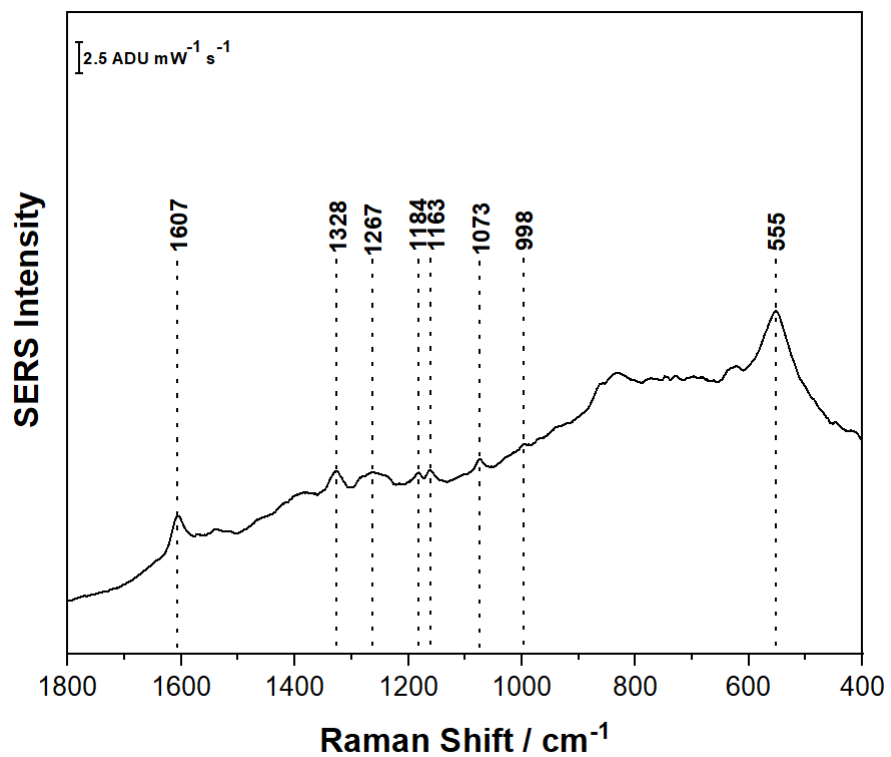


Figure 18. EC-SERS spectra at -0.7 V vs Ag/AgCl for 50 μL of 1 mg mL^{-1} cortisol deposited onto the fabric chip electrode. The spectrum was acquired at 785 nm excitation for 30 seconds at a laser power of 42.6 mW.

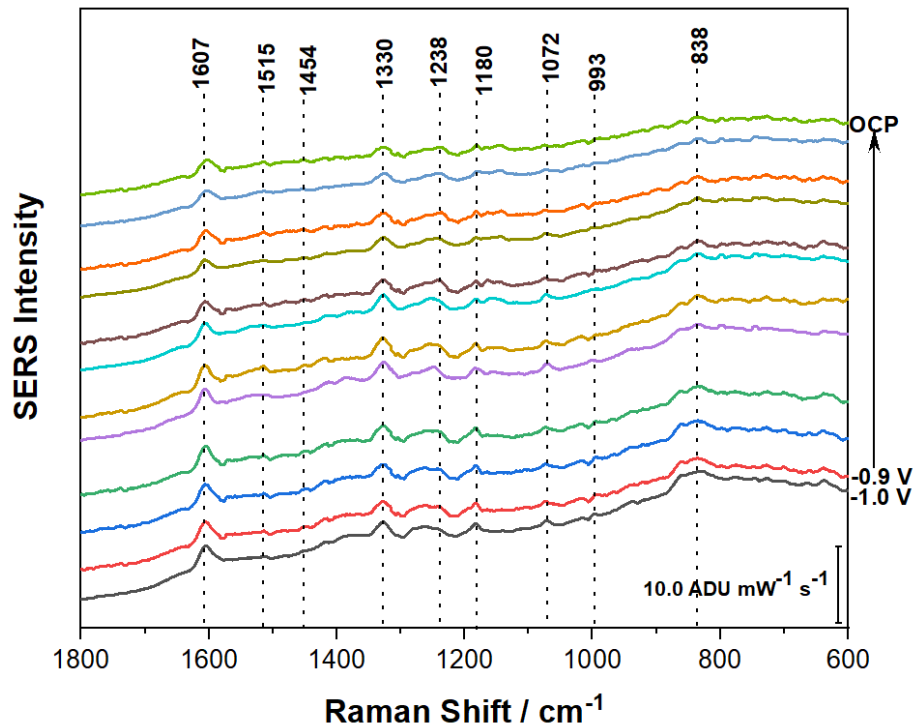


Figure 19. Anodic EC-SERS progression for 50 μL of 1.0 mg mL^{-1} cortisol deposited on the fabric chip electrode. The spectra were acquired at 785 nm excitation for 30 seconds at a laser power of 42.6 mW.

The cortisol peaks were clearly detected in the 800 to 1640 cm^{-1} region in the EC-SERS spectra. The observable peaks are highlighted in Table 2 and Table 3, are consistent with the cortisol Raman peaks (Cortisol-Raman-Spectrum-Spectrabase) and cortisol SERS peaks reported in studies by TJ Moore (Moore and Sharma 2020). The peak observed at 1607 cm^{-1} corresponds to the C=C bond, peaks in the range of 1000 to 600 cm^{-1} corresponds the cholesterol skeleton in the cortisol molecule. The C-C-C asymmetric stretch gives rise to the peak at 1329 cm^{-1} . Peaks observed at 1266 cm^{-1} occurs due to the bend in CH, CH₂ and OH (alcohol functional group). A bend in CH, OH group and a twist in CH₂ gives rise to the peak observed at 1163 cm^{-1} . Peak at 1183 cm^{-1} is observed because of the alicyclic carbon chain. Cortisol molecules have asymmetric stretch band in ring which give rise to peak at 1075 cm^{-1} .

Table 2. Peaks reported for 50 μL of 1 mg/mL cortisol in cathodic region and -0.7 V vs Ag/AgCl. These peaks are consistent with the reported Raman peaks (Cortisol-Raman-Spectrum-Spectrabase) and SERS peaks for cortisol (Moore and Sharma 2020).

Peaks Observed in Cathodic Progression (cm^{-1})	Peaks Observed at -0.7V vs Ag/AgCl (cm^{-1})	Raman Reference Peak (cm^{-1}) (Cortisol-Raman-Spectrum-Spectrabase)	TJ Moore SERS Reference Peak (cm^{-1}) (Moore and Sharma 2020)	Vibrational modes (Moore and Sharma 2020)
1606	1607	1610	1609	C=C stretch
1390			1378	CH ₃ symmetric bend + CH wag + OH wag (C ring)
1329	1328	1330	1330	C-C-C asymmetric stretch A ring
1266	1267	1270	1269	CH bend + CH ₂ bend + OH bend
1183	1184	1175		Alicyclic carbon chain
1163		1175	1149	CH ₂ twist + CH bend + OH bend
1075	1073	1060	1073	Asymmetric ring breathing (C ring)
995	998	990		Cholesterol skeleton
550	555	545		Cholesterol skeleton

Table 3. Peaks reported for 50 μL of 1 mg/mL cortisol in anodic region and -0.8V vs Ag/AgCl. These peaks are consistent with the reported Raman and SERS peaks for cortisol (Moore and Sharma 2020) (Cortisol-Raman-Spectrum-Spectrabase).

Peaks Observed in Anodic Progression (cm^{-1})	Peaks Observed at -0.8V vs Ag/AgCl (cm^{-1})	Raman Reference Peak (cm^{-1}) (Cortisol-Raman-Spectrum-Spectrabase)	TJ Moore EC-SERS Reference Peak (cm^{-1}) (Moore and Sharma 2020)	Raman Band Assignment (Moore and Sharma 2020)
1607	1606	1610	1609	C=C stretch
1515	1514		1504	
1454	1450	1450	1448	CH ₂ scissor (D ring + pendant)
1330	1330	1330	1330	C-C-C asymmetric stretch A ring
1238	1242	1240	1239	C-C-C asymmetric stretch (C ring)
1180	1183	1175		Alicyclic carbon chain
1072	1075	1060	1073	Asymmetric ring breathing (C ring)
993	997	985		Cholesterol skeleton
838	839			Cholesterol skeleton

Cortisol is a hydrophobic molecule. Addition of supporting electrolyte NaF allows signal peaks to be seen at OCP. The addition of 0.1 M NaF as the supporting electrolyte allows cortisol molecules to come closer to the metal surface and avoid the aqueous bulk. This allows for signal peaks to be observed at OCP. On application of negative voltage, the cortisol molecule comes closer to metal surface and signal intensity increases with an increase in application of negative voltage. As shown in Figure 20, the -0.7 V signal exhibits stronger peaks as compared to the OCP for cortisol.

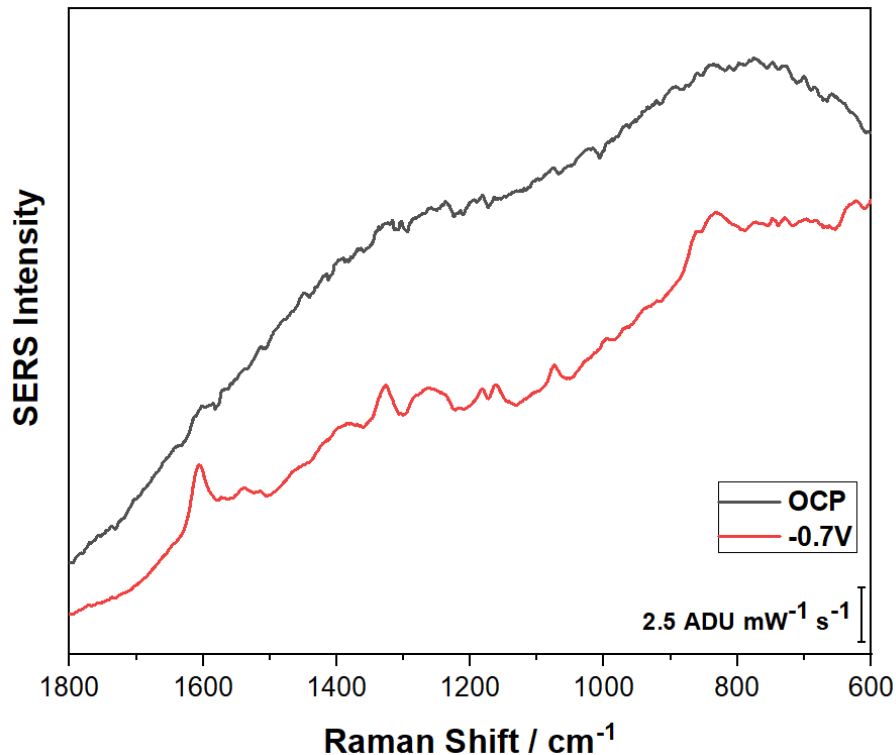


Figure 20. Comparison of OCP and -0.7 V signal peaks for 50 μL of 1.0 mg mL^{-1} cortisol deposited on the fabric chip electrode. The spectra were acquired at 785 nm excitation for 30 seconds at a laser power of 42.6 mW.

To ensure the reproducibility of the fabric sensor and its ability to detect cortisol, a replicate experiment was conducted with 50 μL of 1.0 mg mL^{-1} cortisol. Figures 21 and 22 show the cathodic and anodic progression for replicate EC-SERS studies for 50 μL cortisol, respectively. In Figure 21, a background signal can be seen for 0.0 V and OCP. This may occur because of the background fluorescence from cortisol. Figure 23 shows a comparison of EC-SERS progression replicative studies at -0.7V Ag/AgCl for 50 μg of 1.0 mg mL^{-1} cortisol. The peak intensity for both trials shows a significant variance which indicates the fabric sensor does not provide reproducible signal. Signal reproducibility of the fabric sensor may be affected due to several factors such as the thickness of the electrodes on the sensor; application of voltage may result in breaking carbon ink imprinted on electrodes; a too thick layer of nail polish can affect the flow of current; poor

adhesion of the silver nanoparticles on the carbon ink of working electrode may also affect the reproducibility of the fabric sensor. Future studies should focus on increasing the adhesion between the silver nanoparticles and carbon ink on the working electrode, improving adhesion of cortisol on the silver nanoparticles and improving the reproducibility of the fabric sensor.

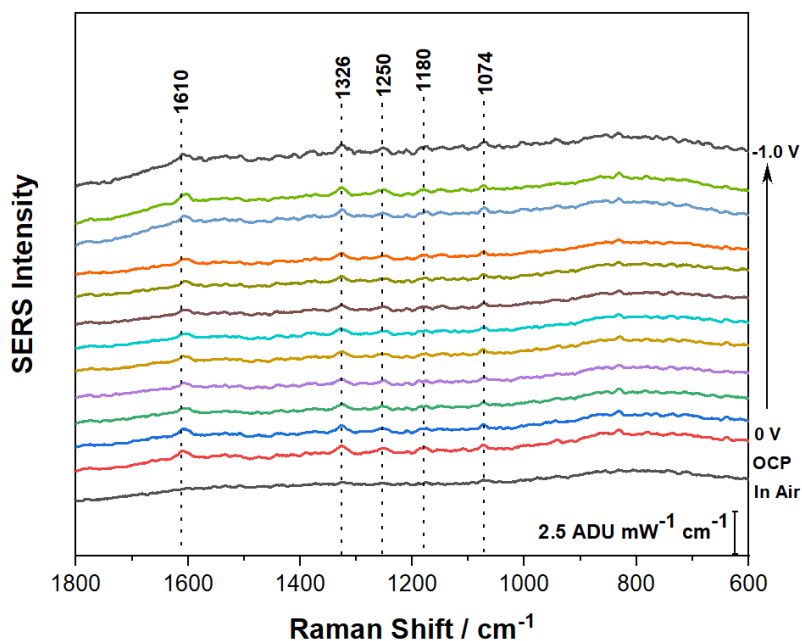


Figure 21. Cathodic EC-SERS progression for 50 μL of 1.0 mg mL^{-1} cortisol deposited on the fabric chip electrode. The spectra were acquired at 785 nm excitation for 30 seconds at a laser power of 42.6 mW.

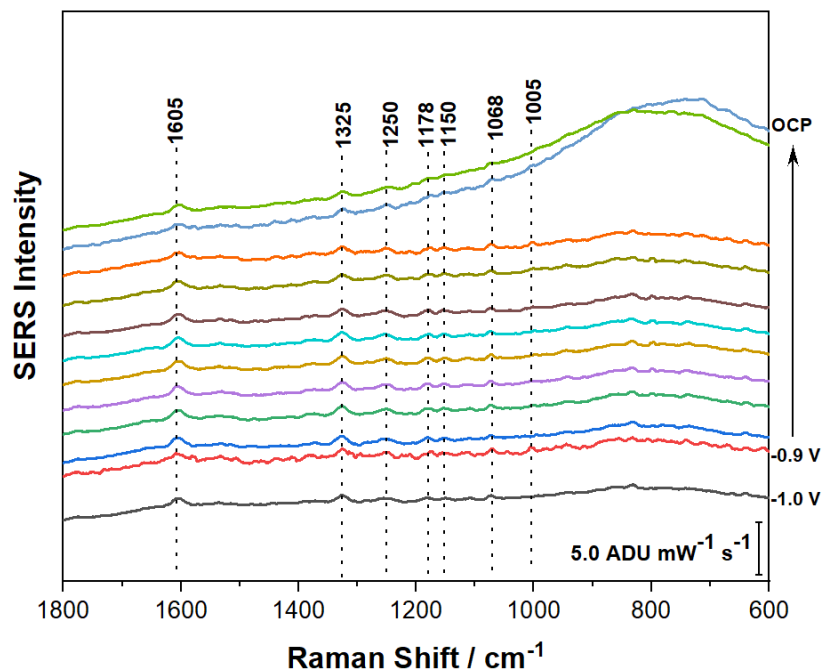


Figure 22. Anodic EC-SERS progression for 50 μL of 1.0 mg mL^{-1} cortisol deposited on the fabric chip electrode. The spectra were acquired at 785 nm excitation for 30 seconds at a laser power of 42.6 mW.

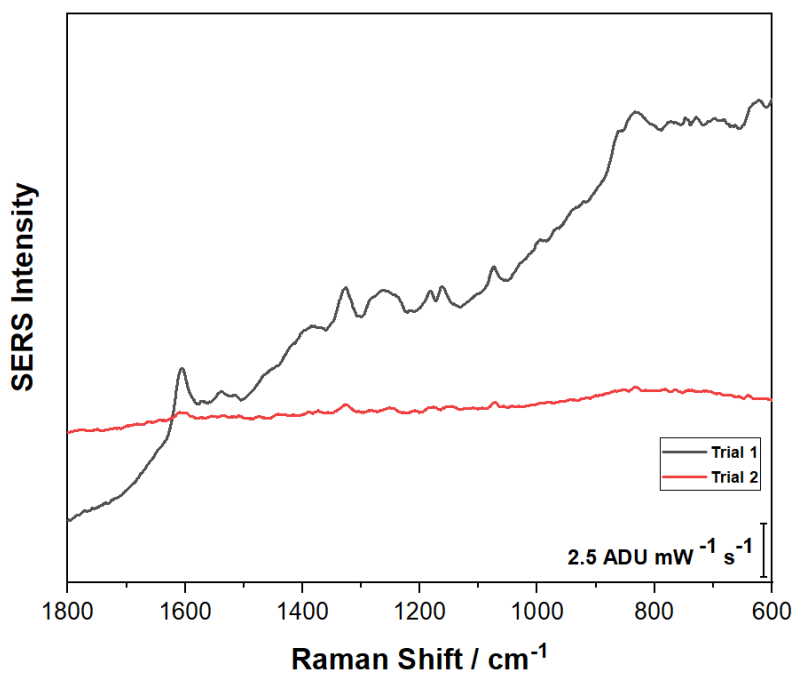


Figure 23. Comparison of EC-SERS progression at -0.7V Ag/AgCl for 50 μg of 1.0 mg mL^{-1} replicate cortisol trials deposited on the fabric chip electrode. The spectra were acquired at 785 nm excitation for 30 seconds at a laser power of 42.6 mW.

As shown in figure 24, 25 and 26, EC-SERS studies were also conducted using 65 μL , 75 μL and 100 μL of 1.0 mg mL^{-1} cortisol deposited on the fabric chip electrode, respectively. The intensity of signal peaks increases with an increase in negative voltage. EC-SERS studies for 100 μL of 1.0 mg mL^{-1} cortisol shows low signal peak intensity as compared to EC-SERS plot for 65 μL and 75 μL of 1.0 mg mL^{-1} cortisol. This may have resulted either because of using lower laser power and reduced integration time for 100 μL of 1.0 mg mL^{-1} cortisol studies or the sample being saturated.

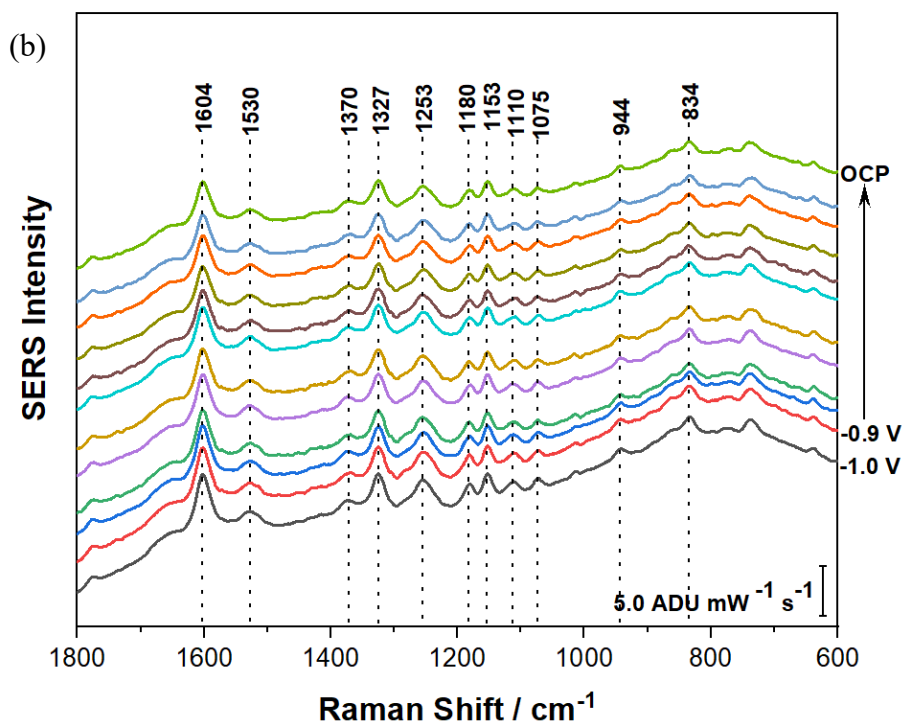
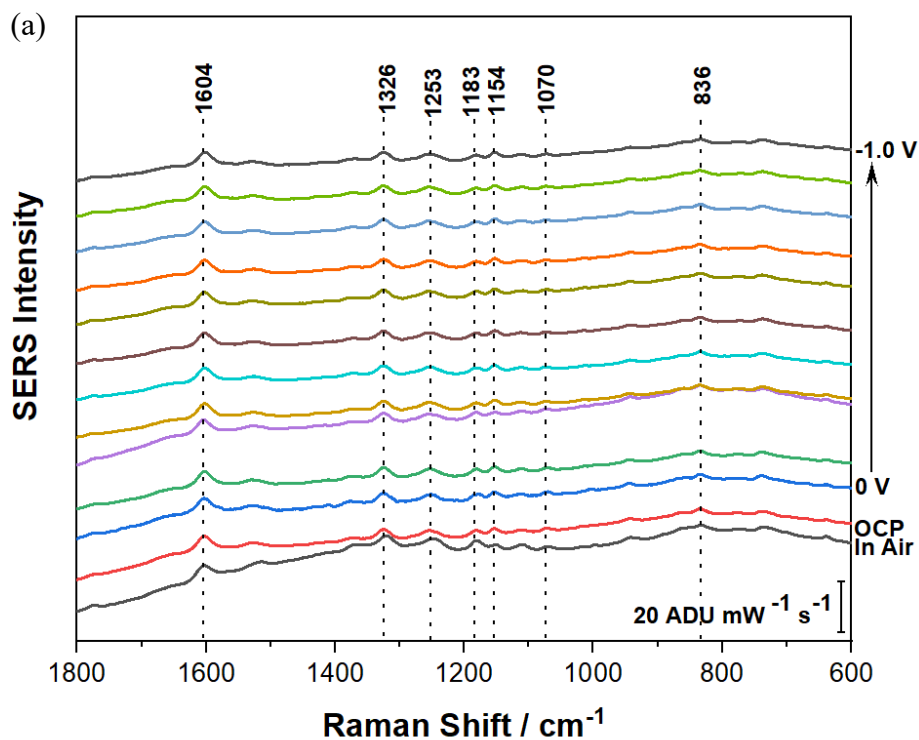


Figure 24. (a) Cathodic (b) Anodic EC-SERS progression for 65 μL of 1.0 mg mL^{-1} cortisol deposited on the fabric chip electrode. The spectra were acquired at 785 nm excitation for 30 seconds at a laser power of 42.6 mW.

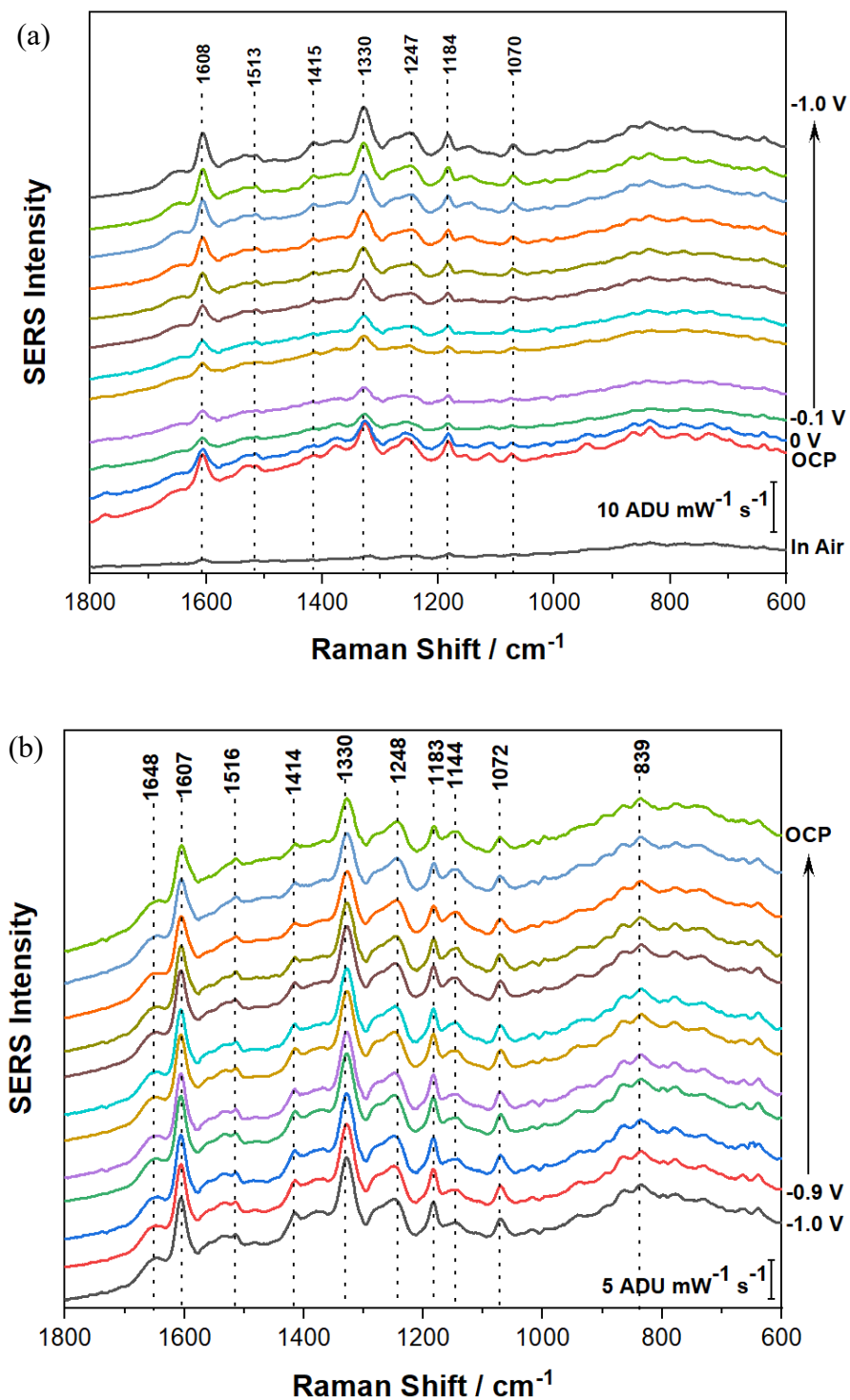


Figure 25. (a) Cathodic (b) Anodic EC-SERS progression for 75 μL of 1.0 mg mL^{-1} cortisol deposited on the fabric chip electrode. The spectra were acquired at 785 nm excitation for 30 seconds at a laser power of 42.6 mW.

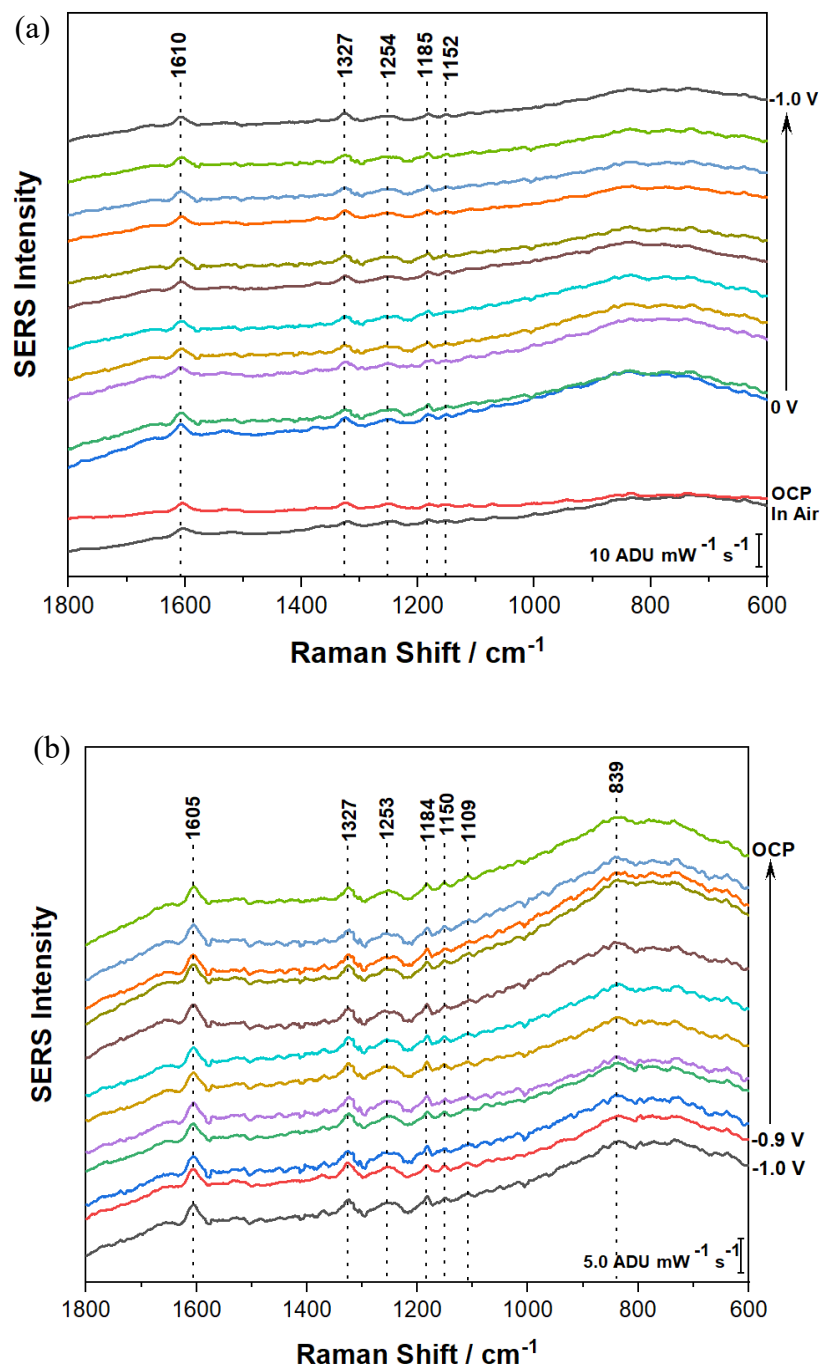


Figure 26. (a) Cathodic (b) Anodic EC-SERS progression for 100 μL of 1.0 mg mL^{-1} cortisol deposited on the fabric chip electrode. The spectra were acquired at 785 nm excitation for 15 seconds at a laser power of 29.3 mW.

For performing EC-SERS for 100 μL of 1.0 mg mL^{-1} cortisol, the spectra were acquired for 15 seconds at a laser power of 29.3 mW instead of 30 seconds at a laser power of 42.6 mW. The spectra showed saturation at 42.6 mW. Thus, reducing the integration time and power of laser allowed for collection of the spectra for 100 μL cortisol.

Additional EC-SERS cortisol studies were performed using three different volumes of 1.0 mg mL^{-1} cortisol (65 μL , 75 μL and 100 μL) to show the correlation between cortisol volume and peak intensity. However, these concentrations are not biologically relevant with clinical cortisol concentration. These experimental studies help to prove the concept of being able to use EC-SERS and fabric chip to detect cortisol. As seen in Figure 27, the intensity of the cortisol signal increases with an increase in the volume of cortisol deposited on the fabric electrode chip. With an increase in the amount of cortisol deposited on the fabric sensor, the peak intensity also increased. This confirms that the sensor can be used to detect the concentration of cortisol in human body under stress. The peak intensity increased for 65 μL and 75 μL of 1.0 mg mL^{-1} cortisol. However, 100 μL of 1.0 mg mL^{-1} cortisol shows a lower peak intensity as compared to 65 μL and 75 μL of 1.0 mg mL^{-1} cortisol. This might be because of the sample being saturated or using a lower laser power. Decreasing the laser power and integration time can result in reduced peak intensity. Reducing the integration time increases the signal to noise ratio.

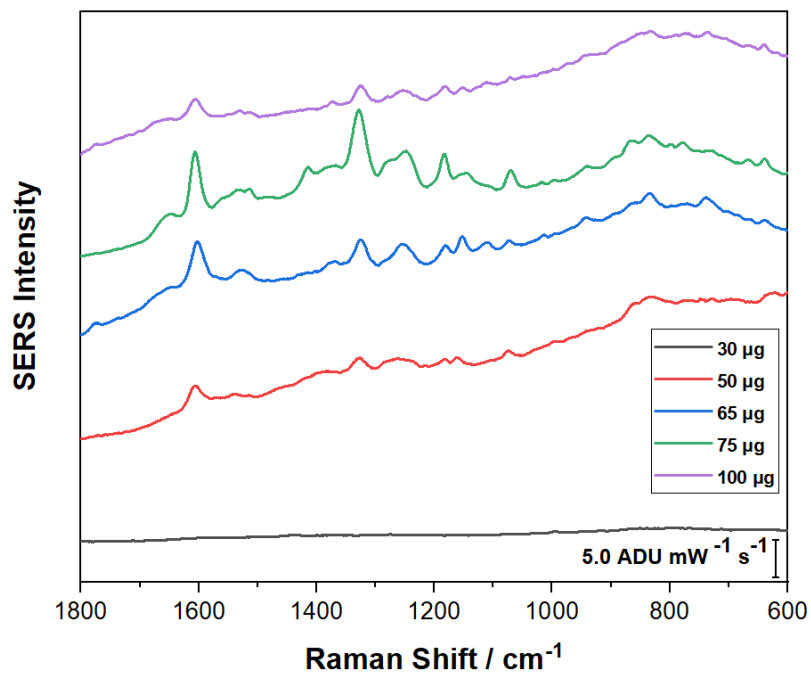


Figure 27. Comparison of EC-SERS progression at -0.7V Ag/AgCl for 30, 50, 65, 75 and 100 μL of 1.0 mg mL^{-1} cortisol deposited on the fabric chip electrode. The spectra were acquired at 785 nm excitation for 30 seconds at a laser power of 42.6 mW.

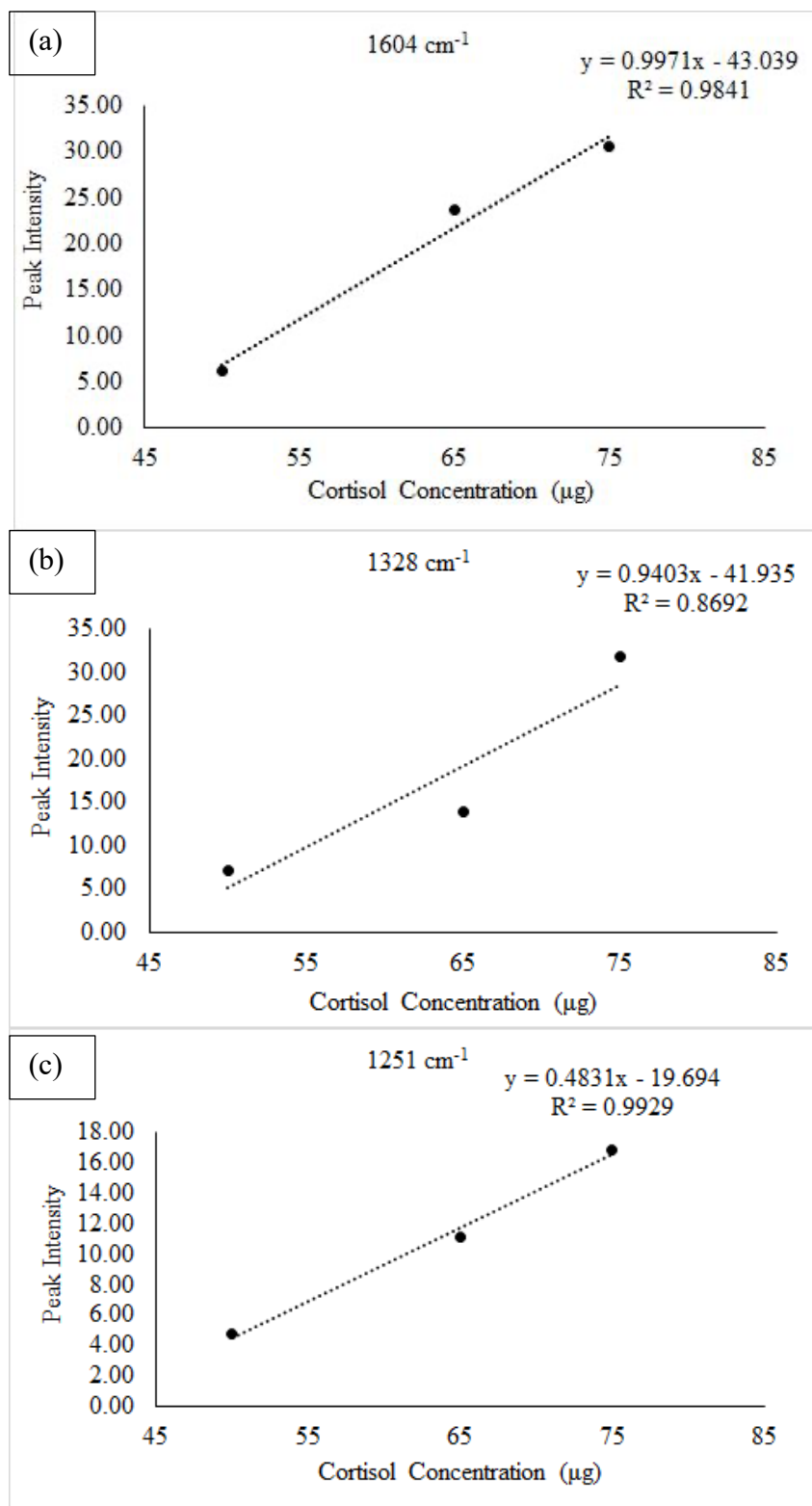


Figure 28. Linear trendline in peak intensity for peaks (a) 1604 cm^{-1} (b) 1328 cm^{-1} (c) 1251 cm^{-1} for 50, 65 and 75 μg of 1.0 mg mL^{-1} cortisol.

Figure 28 shows a linear trend for 1604 cm^{-1} , 1328 cm^{-1} and 1251 cm^{-1} peaks when peak intensity is plotted for 50, 65 and 75 μg of 1.0 mg mL^{-1} cortisol. It indicates that the cortisol peak intensity increases with an increase in the amount of cortisol.

4 CONCLUSION AND FUTURE WORK

Early diagnosis of PTSD is challenging. Demand for detecting biomarkers for diagnosis at the point of care has increased. Fabric sensors can help in the early diagnosis of PTSD in a timely and effective way. In this work, Electrochemical Surface Enhanced Raman Spectroscopy (EC-SERS) using a fabric-based sensor was explored for the detection of cortisol for early diagnosis of PTSD.

Cortisol is a glucocorticoid stress hormone. It has a planar structure and is hydrophobic which makes it a challenging molecule to be detected via EC-SERS as its ability to adhere to silver nanoparticles is poor. Silver and carbon conductive inks were traced onto a blend fabric (37% silk, 35% hemp, 28% organic cotton) to prepare the fabric sensor. Counter, working and reference electrodes were traced with silver conductive ink, and the working and reference electrode were traced with carbon ink on top of silver conductive ink. The silver nanoparticles were drop coated on the working electrode. The fabric sensor was optimized by mercerizing it to increase the dye ability and keep the carbon ink intact on the fabric. Moreover, a thin layer of transparent nail polish was applied on the upper half of the fabric to prevent short circuiting as the supporting electrolyte will not reach the top of fabric touching cables.

The main objective of this study was to develop a functional fabric sensor and utilize it to detect cortisol by performing EC-SERS. The fabric sensor was characterized via EC-SERS, UV-vis spectroscopy, cyclic voltammetry (CV), and scanning electron microscopy (SEM). An LSPR band at 394 nm was observed in the UV-vis spectrum for the silver nanoparticles. This result indicates that the colloidal AgNPs synthesized in this project are of an appropriate size (~30 nm diameter) and are nearly monodisperse in terms of size and shape. Analysis of SEM sample using ImageJ software indicated the size of these silver nanoparticles was approximately $27.5 \text{ nm} \pm 4$

nm in diameter. The fabric sensor was characterized by cyclic voltammetry first, followed by performing EC-SERS study using 10 μL of 1.0 mM *p*-ATP as a probe. The *p*-ATP signal was observable and the fabric sensor was found to be functional.

To test the research hypothesis, initial EC-SERS studies were performed with 30 μL of 1.0 mg mL⁻¹ cortisol; unfortunately the signal intensity was too weak to be detected. Therefore, EC-SERS studies were conducted with 50 μL of 1.0 mg mL⁻¹ cortisol. Strong intense cortisol peaks were observed. A replicate study was also performed with 50 μL of 1.0 mg mL⁻¹ cortisol and cortisol peaks were observable, however the signal intensity was significantly different suggesting that the fabric sensor is not reproducible. Cortisol peaks were observed in the 800 to 1640 cm⁻¹ region at OCP and on applying negative voltage. The intensity of signal peaks increased with an increase in the application of negative voltage. For lower concentrations of cortisol, the signal was only observed under applied voltage. The relationship between cortisol concentration and signal intensity was explored by performing EC-SERS studies with 65 μL , 75 μL , and 100 μL of 1.0 mg mL⁻¹ cortisol. The peak intensity was higher than those observed for 50 μL of 1.0 mg mL⁻¹ cortisol, thus indicating that peak intensity increases with the amount of cortisol deposited on fabric sensor. EC-SERS study for 100 μL of 1.0 mg mL⁻¹ cortisol showed saturation when spectra were acquired at 785 nm excitation for 30 seconds at a laser power of 42.6 mW. Therefore, the integration time was reduced to 15 seconds, and laser power was reduced to 29.3 mW. This resulted in lower peak intensity of cortisol for the highest concentration studied.

This thesis work explored the development of a functional fabric sensor for use as an EC-SERS substrate to detect biomarkers for PTSD, with a goal towards integration into a wearable sensor. Future work should focus on ensuring reproducibility of the fabric sensor. EC-SERS studies should be conducted with a lower and higher concentration of cortisol. After exploring EC-

SERS studies with cortisol, EC-SERS studies should be conducted to detect other biomarkers for PTSD such as dehydroepiandrosterone. Future work should also focus on re-usability, launderability, and biocompatibility of the fabric sensor.

5 APPENDIX

5.1 Copyright of Figures Used

Copyright for Figure 3



Reusable Surface-Enhanced Raman Spectroscopy Membranes and Textiles via Template-Assisted Self-Assembly and Micro/Nanoimprinting
Author: Aditya Garg, Wonil Nam, Wei Zhou
Publication: Applied Materials
Publisher: American Chemical Society
Date: Dec 1, 2020
Copyright © 2020, American Chemical Society

PERMISSION/LICENSE IS GRANTED FOR YOUR ORDER AT NO CHARGE


This type of permission/license, instead of the standard Terms and Conditions, is sent to you because no fee is being charged for your order. Please note the following:

- Permission is granted for your request in both print and electronic formats, and translations.
- If figures and/or tables were requested, they may be adapted or used in part.
- Please print this page for your records and send a copy of it to your publisher/graduate school.
- Appropriate credit for the requested material should be given as follows: "Reprinted (adapted) with permission from {COMPLETE REFERENCE CITATION}. Copyright {YEAR} American Chemical Society." Insert appropriate information in place of the capitalized words.
- One-time permission is granted only for the use specified in your RightsLink request. No additional uses are granted (such as derivative works or other editions). For any uses, please submit a new request.

If credit is given to another source for the material you requested from RightsLink, permission must be obtained from that source.

[BACK](#) [CLOSE WINDOW](#)

Copyright for Figure 4



A Wearable Surface-Enhanced Raman Scattering Sensor for Label-Free Molecular Detection
Author: Eun Hye Koh, Won-Chul Lee, Yeong-Jin Choi, et al
Publication: Applied Materials
Publisher: American Chemical Society
Date: Jan 1, 2021
Copyright © 2021, American Chemical Society

PERMISSION/LICENSE IS GRANTED FOR YOUR ORDER AT NO CHARGE

This type of permission/license, instead of the standard Terms and Conditions, is sent to you because no fee is being charged for your order. Please note the following:

- Permission is granted for your request in both print and electronic formats, and translations.
- If figures and/or tables were requested, they may be adapted or used in part.
- Please print this page for your records and send a copy of it to your publisher/graduate school.
- Appropriate credit for the requested material should be given as follows: "Reprinted (adapted) with permission from {COMPLETE REFERENCE CITATION}. Copyright {YEAR} American Chemical Society." Insert appropriate information in place of the capitalized words.
- One-time permission is granted only for the use specified in your RightsLink request. No additional uses are granted (such as derivative works or other editions). For any uses, please submit a new request.

If credit is given to another source for the material you requested from RightsLink, permission must be obtained from that source.

[BACK](#) [CLOSE WINDOW](#)

5.2 Appendix Tables

Appendix Table A1. For 20 silver nanoparticles, measured diameter reported along with its mean and standard deviation using ImageJ software.

Nanoparticle	Diameter (nm)
1	25.8
2	30.8
3	31.2
4	29.7
5	24.6
6	31.5
7	33.3
8	24.4
9	27.8
10	20.1
11	26.5
12	26.3
13	23.4
14	23.7
15	26.7
16	26.6
17	24.7
18	25.2
19	31.6
20	36.2
Mean	27.5
SD	4.0

Appendix Table A2. Calculated difference between y-axis value and baseline value for the reported cortisol peaks in (A) Cathodic progression (B) -0.7V vs Ag/AgCl of cathodic progression (C) -0.8V vs Ag/AgCl of cathodic progression (D) Anodic progression -0.8V vs Ag/AgCl of anodic progression

(A)

Cathodic Progression								
Peaks (cm^{-1})→	1606	1390	13229	1266	1183	1075	995	550
y coordinate of peak ($\text{mW}^{-1}\text{s}^{-1}$)	90.5	79.5	89.9	94.3	94.7	90.9	96.2	88.4
Baseline value ($\text{mW}^{-1}\text{s}^{-1}$)	87.8	78.9	88.2	92.7	92.5	90.3	94.6	83.7
Difference ($\text{mW}^{-1}\text{s}^{-1}$)	2.6	0.6	1.7	1.6	2.2	0.6	1.5	4.7

(B)

-0.7V vs Ag/AgCl								
Peaks (cm^{-1}) \rightarrow	1607	1328	1267	1184	1163	1073	998	555
y coordinate of peak ($\text{mW}^{-1}\text{s}^{-1}$)	8.9	12.4	12.3	12.4	12.6	13.5	14.7	25.6
Baseline value ($\text{mW}^{-1}\text{s}^{-1}$)	7.1	10.5	11.1	11.4	11.5	12.7	14.1	20.6
Difference ($\text{mW}^{-1}\text{s}^{-1}$)	1.8	2.0	1.2	1.0	1.1	0.8	0.7	4.9

(C)

-0.1V vs Ag/AgCl				
Peaks (cm^{-1}) \rightarrow	1603	1353	1244	1157
y coordinate of peak ($\text{mW}^{-1}\text{s}^{-1}$)	3.7	8.1	8.4	8.5
Baseline value ($\text{mW}^{-1}\text{s}^{-1}$)	2.5	6.4	6.9	7.4
Difference ($\text{mW}^{-1}\text{s}^{-1}$)	1.2	1.8	1.5	1.2

(D)

Anodic Progression										
Peaks (cm ⁻¹)→	1607	1515	1454	1330	1238	1180	1072	993	838	
y coordinate of peak (mW ⁻¹ s ⁻¹)	92.9	47.5	93.2	88.1	80.0	95.0	60.1	18.6	18.4	
Baseline value (mW ⁻¹ s ⁻¹)	91.5	46.5	92.5	86.8	78.8	93.6	58.9	16.9	15.1	
Difference (mW ⁻¹ s ⁻¹)	1.4	1.0	0.8	1.3	1.3	1.4	1.2	1.6	3.3	

(E)

-0.8 V vs Ag/AgCl										
Peaks (cm ⁻¹)→	1606	1514	1450	1418	1330	1242	1183	1075	997	839
y coordinate of peak (mW ⁻¹ s ⁻¹)	6.6	5.5	6.1	7.2	9.5	8.8	9.2	9.4	10.4	15.1
Baseline value (mW ⁻¹ s ⁻¹)	4.4	4.9	5.5	5.9	7.5	7.4	7.4	8.8	9.3	14.0
Difference (mW ⁻¹ s ⁻¹)	2.2	0.6	0.6	1.3	1.9	1.4	1.8	0.5	1.0	1.1

Appendix Table A3. Coefficient of variation and standard deviation value for the intensity of reported 50 μL of 1.0 mg mL^{-1} cortisol peaks

PEAK (cm^{-1})→	1604	1325	1251	1072
TRIAL 1 Peak Height	6.08	5.01	4.70	2.49
TRIAL 2 Peak Height	9.03	10.95	7.19	6.73
STDV	2.08	4.20	1.76	3.00
Average	7.56	7.98	5.94	4.61
Coefficient of Variation (%)	27.55	52.66	29.63	65.07

6 REFERENCES

Alhatab DS. 2017 Apr. Development of a fabric-based plasmonic sensor for point-of-care diagnostics. Saint Mary's University:145p. Accessed from:
<https://library2.smu.ca/handle/01/27000?show=full>

Apilux A, Rengpipat S, Suwanjang W, and Chailapakul O. 2018. Development of competitive lateral flow immunoassay coupled with silver enhancement for simple and sensitive salivary cortisol detection. EXCLI Journal; 17:Doc1198; ISSN 1611-2156.

Bindesri SD, Alhatab DS, and Brosseau CL. 2018. Development of an electrochemical surface-enhanced Raman spectroscopy (EC-SERS) fabric-based plasmonic sensor for point-of-care diagnostics. Analyst. 143(17):4128–4135.

Chaudhuri S, Thompson H, Demiris G. 2014. Fall Detection Devices and their Use with Older Adults: A Systematic Review. J Geriatr Phys Ther. 37(4):178–196.

Coosemans J, Hermans B, Puers R. 2006. Integrating wireless ECG monitoring in textiles. Sensors and Actuators A: Physical. 130:48–53.

Cortisol - Raman - Spectrum - SpectraBase. [accessed 2022 Jan 15].
<https://spectrabase.com/spectrum/FhOIEJ8nutu>.

Eberling P, Koivisto VA. 1994. Physiological importance of dehydroepiandrosterone. The Lancet. 343(8911):1479–1481.

Fletcher RR, Tam S, Omojola O, Redemske R, Kwan J. 2011. Wearable sensor platform and mobile application for use in cognitive behavioral therapy for drug addiction and PTSD. In: 2011 Annual International Conference of the IEEE Engineering in Medicine and Biology Society. p. 1802–1805.

Gao W, Emaminejad S, Nyein HYY, Challa S, Chen K, Peck A, Fahad HM, Ota H, Shiraki H, Kiriya D, et al. 2016a. Fully integrated wearable sensor arrays for multiplexed in situ perspiration analysis. *Nature*. 529(7587):509–514.

Garg A, Nam W, Zhou W. 2020. Reusable Surface-Enhanced Raman Spectroscopy Membranes and Textiles via Template-Assisted Self-Assembly and Micro/Nanoimprinting. *ACS Appl Mater Interfaces*. 12(50):56290–56299.

Gaskell. 2005. Post-traumatic stress disorder. Gaskell. [accessed 2021 Nov 2]. <https://www.ncbi.nlm.nih.gov/books/NBK56506/>.

Herbert J. 2007. DHEA. In: Fink G, editor. *Encyclopedia of Stress (Second Edition)*. New York: Academic Press. p. 788–791. [accessed 2021 Nov 4].

Jakobsen NA, Hamdy FC, Bryant RJ. 2016. Novel biomarkers for the detection of prostate cancer. *J Clin Urol*. 9(2 Suppl):3–10.

Koh EH, Lee W-C, Choi Y-J, Moon J-I, Jang J, Park S-G, Choo J, Kim D-H, Jung HS. 2021. A Wearable Surface-Enhanced Raman Scattering Sensor for Label-Free Molecular Detection. *ACS Appl Mater Interfaces*. 13(2):3024–3032.

Kravets VG, Kabashin AV, Barnes WL, Grigorenko AN. 2018. Plasmonic Surface Lattice Resonances: A Review of Properties and Applications. *Chem Rev*. 118(12):5912–5951.

Marques MRC, Loebenberg R, Almukainzi M. 2011. Simulated Biological Fluids with Possible Application in Dissolution Testing. *Dissolution Technol*. 18(3):15–28.

McKay LI, Cidlowski JA. 2003. Pharmacokinetics of Corticosteroids. *Holland-Frei Cancer Medicine 6th edition*. [accessed 2021 Nov 2].

Miao X-R, Chen Q-B, Wei K, Tao K-M, Lu Z-J. 2018. Post traumatic stress disorder: from diagnosis to prevention. *Mil Med Res.* 5:32.

Michopoulos V, Norrholm SD, Jovanovic T. 2015a. Diagnostic Biomarkers for Posttraumatic Stress Disorder: Promising Horizons from Translational Neuroscience Research. *Biol Psychiatry.* 78(5):344–353.

Moore TJ, Sharma B. 2020. Direct Surface Enhanced Raman Spectroscopic Detection of Cortisol at Physiological Concentrations. *Anal Chem.* 92(2):2052–2057.

Mugo SM, Alberkant J. 2020. Flexible molecularly imprinted electrochemical sensor for cortisol monitoring in sweat. *Anal Bioanal Chem.* 412(8):1825–1833.

Naseri M, Ziora ZM, Simon GP, Batchelor W. 2022. ASSURED-compliant point-of-care diagnostics for the detection of human viral infections. *Reviews in Medical Virology.* 32(2):e2263.

Pelton M, Aizpurua J, Bryant G. 2008. Metal-nanoparticle plasmonics. *Laser & Photon Rev.* 2(3):136–159.

Post-traumatic stress disorder (PTSD) - Symptoms and causes. 2018 July 6. Mayo Clinic. [accessed 2021 Nov 2]. <https://www.mayoclinic.org/diseases-conditions/post-traumatic-stress-disorder/symptoms-causes/syc-20355967>.

Robinson AM, Zhao L, Alam MYS, Bhandari P, Harroun SG, Dendukuri D, Blackburn J, Brosseau CL. 2015. The development of “fab-chips” as low-cost, sensitive surface-enhanced Raman spectroscopy (SERS) substrates for analytical applications. *Analyst.* 140(3):779–785.

Schmidt U, Kaltwasser SF, Wotjak CT. 2013. Biomarkers in Posttraumatic Stress Disorder: Overview and Implications for Future Research. *Disease Markers.* 35(1):43–54.

Sharma B, Frontiera RR, Henry A-I, Ringe E, Van Duyne RP. 2012a. SERS: Materials, applications, and the future. *Materials Today*. 15(1–2):16–25.

Sharma S, Zapatero-Rodríguez J, Estrela P, O’Kennedy R. 2015a. Point-of-Care Diagnostics in Low Resource Settings: Present Status and Future Role of Microfluidics. *Biosensors (Basel)*. 5(3):577–601.

Soldin SJ, Wong, Edward C, Brugnara, Carlo, Solden OP, American Association for Clinical Chemistry. 2011. Pediatric reference intervals.

Sonntag MD, Klingsporn JM, Zrimsek AB, Sharma B, Ruvuna LK, Van Duyne RP. 2014. Molecular plasmonics for nanoscale spectroscopy. *Chem Soc Rev*. 43(4):1230–1247.

Strimbu K, Tavel JA. 2010. What are Biomarkers? *Curr Opin HIV AIDS*. 5(6):463–466.

Thau L, Gandhi J, Sharma S. 2021. Physiology, Cortisol. In: *StatPearls*. Treasure Island (FL): StatPearls Publishing. [accessed 2021 Nov 2].

Van Ameringen M, Mancini C, Patterson B, Boyle MH. 2008. Post-traumatic stress disorder in Canada. *CNS Neurosci Ther*. 14(3):171–181.

Waller DG, Sampson AP. 2018. 44 - Corticosteroids (glucocorticoids and mineralocorticoids). In: Waller DG, Sampson AP, editors. *Medical Pharmacology and Therapeutics (Fifth Edition)*. Elsevier. p. 503–511. [accessed 2021 Nov 2].

Wang B, Zhao C, Wang Z, Yang K-A, Cheng X, Liu W, Yu W, Lin S, Zhao Y, Cheung KM, et al. 2022. Wearable aptamer-field-effect transistor sensing system for noninvasive cortisol monitoring. *Science Advances*. 8(1):eabk0967.

Wang Y, Zhao C, Wang J, Luo X, Xie L, Zhan S, Kim J, Wang X, Liu X, Ying Y. Wearable plasmonic-metasurface sensor for noninvasive and universal molecular fingerprint detection on biointerfaces. *Science Advances*. 7(4):eabe4553.

Xu K, Zhou R, Takei K, Hong M. 2019. Toward Flexible Surface-Enhanced Raman Scattering (SERS) Sensors for Point-of-Care Diagnostics. *Advanced Science*. 6(16):1900925.

Yehuda R, Brand SR, Golier JA, Yang R-K. 2006. Clinical correlates of DHEA associated with post-traumatic stress disorder. *Acta Psychiatr Scand*. 114(3):187–193.

Young A. 1995. Reasons and Causes for Post-Traumatic Stress Disorder. *Transcultural Psychiatric Research Review*. 32(3):287–298.

Zhao L, Blackburn J, Brosseau CL. 2015. Quantitative detection of uric acid by electrochemical-surface enhanced Raman spectroscopy using a multilayered Au/Ag substrate. *Anal Chem*. 87(1):441–447.